arXiv:astro-ph/0306356v1 18 Jun 2003

RR Lyrae stars in Galactic globular clusters. II. A theoretical approach to variables in M3

Marconi, M.[1], Caputo, F.[2], Di Criscienzo, M.[1], and Castellani, M.[2]

ABSTRACT

We present predicted relations connecting pulsational (period and amplitude of pulsation) and evolutionary (mass, absolute magnitude and color) parameters, as based on a wide set of convective pulsating models of RR Lyrae stars with Z=0.001, Y=0.24 and mass and luminosity suitable for the "old" (age $>$ 8 Gyr) variables observed in globular clusters. The relations are collated with sound constraints on the mass of pulsators, as inferred from up-to-date evolutionary models of horizontal branch stars, in order to provide a self-consistent theoretical framework for the analysis of observed variables. The theoretical predictions are tested through a detailed comparison with measurements of RR Lyrae stars in the globular cluster M3. We show that the predicted relations satisfy a variety of observed data, thus providing a *pulsational* route to the determination of accurate distances to RR Lyrae-rich globular clusters with intermediate metal content. We show that current uncertainties on the intrinsic luminosity of up-to-date horizontal branch models, as due to the input physics used in the computations by the different authors, have a quite low influence ($\sim$ 0.02-0.03 mag) on the pulsational distance modulus. On the contrary, the effect of the different bolometric corrections adopted to convert bolometric luminosity into absolute magnitude is of the order of $\sim$ 0.05-0.06 mag. The pulsation models are also used to perform some valuable tests on the physics adopted in current stellar evolution computations. We show that the constraints inferred by pulsation theory support the large value of the mixing-length parameter (l/H_p=1.9-2.0) adopted to fit observed Red Giant Branches, but, at the same time, they would yield that the luminosity of the horizontal branch updated models is too bright by $\sim$ 0.08±0.05 mag, if helium and metal diffusion is neglected. Conversely, if element diffusion is properly taken into account, then

---

[1] INAF - Osservatorio Astronomico di Capodimonte, via Moiarello 16, I-80131 Napoli, Italy; marcella@na.astro.it, dicrisci@na.astro.it

[2] INAF - Osservatorio Astronomico di Roma, Via di Frascati, 33, I-00040 Monte Porzio Catone Italy; caputo,mkast@coma.mporzio.astro.it

there is a marginal discrepancy of $\sim 0.04\pm0.05$ mag between evolutionary and pulsational predictions.

Subject headings: Stars: evolution - stars: horizontal branch - stars: variables: RR Lyrae

1. Introduction

Radial pulsating variables, whether they are Population I or Population II stars, are of great relevance in several fields of modern astrophysics. In particular, RR Lyrae variables are widely used, via the calibration of their absolute visual magnitude M_V(RR) in terms of the iron-to-hydrogen content [Fe/H], as standard candles for distance determination in the Local Group. On this basis, they provide an independent test of the Cepheid distance scale for nearby galaxies (Magellanic Clouds, M31) as well as a calibration of secondary distance indicators (e.g., the globular cluster luminosity function) in external galaxies, thus yielding relevant clues about the value of the Hubble constant. On the other hand, since the absolute magnitude of the globular cluster main sequence turn-off is a classical "clock" to estimate the age of these ancient stellar systems, one easily understands the relevance of an accurate RR Lyrae distance scale for cosmological studies.

Accordingly, a huge amount of work has been made in the last years to establish the absolute magnitude of Horizontal Branch (HB) stars, and particularly of RR Lyrae variables, and its dependence on the star metal content. Unfortunately, a general consensus has not been achieved yet, leading to the well-known debate between the so-named "short" and "long" distance scale.

On the observational side (e.g., Baade-Wesselink method, Hipparcos and statistical parallax), the estimates of M_V(RR) suggest relatively faint magnitudes, although leaving significant uncertainties (> 0.1 mag, see Vandenberg et al. 2000, hereafter VDB, and references therein). As a matter of example, in the recent review by Cacciari (1999) the empirical values of M_V(RR) at [Fe/H]$=-1.6$ actually range from ~ 0.4 to ~ 0.7 mag. Moreover, it should be mentioned that Fernley et al. (1998) and Groenewegen & Salaris (1999), by assuming the same slope ΔM_V(RR)/Δ [Fe/H]=0.18 mag/dex, give respectively M_V(RR)=0.78$\pm$0.15 mag and 0.50$\pm$0.26 mag at [Fe/H]$=-1.5$, as derived from an identical sample of variables but using statistical parallaxes or reduced parallaxes, respectively. In reality, not only the zero-point but also the slope of the M_V(RR)-[Fe/H] relation is matter of considerable debate and in the relevant literature one finds values in the range of ~ 0.13 to ~ 0.30 mag/dex.

As for the theoretical studies based on HB models, all recent computations that adopt up-to-date physics suggest absolute magnitudes which are somehow brighter than empirical estimates, at fixed [Fe/H]. However, evolutionary predictions themselves, as provided by the various researchers, still suggest significant discrepant (both in the zero-point and the slope) M_V(RR)-[Fe/H] relations (see VDB; Caputo et al. 2000 and references therein). On this issue, it should be noted that HB evolutionary models provide a relation between the bolometric luminosity L and the overall metallicity Z. Thus, any comparison among the various evolutionary predicted M_V(RR)-[Fe/H] relations is affected by two factors of critical importance: a) the conversion of bolometric luminosity and effective temperature into magnitude and color, i.e. the adopted bolometric correction and temperature-color transformation, and b) the scaling between the theoretical Z and the measured [Fe/H] value, i.e. the adopted ratio between α-elements and iron. These factors are still more important when theoretical predictions are compared with observed quantities. In addition, we wish also to mention that the constraints inferred by evolutionary models refer to "*static*" stars, whereas the RR Lyrae observed magnitudes are "*mean*" quantities averaged over the pulsation cycle, which not necessarily are exactly alike static values.

In this context, it is of great help to consider simultaneously the double nature of RR Lyrae stars - from one side, radial pulsators, from the other one, low-mass ($M \leq 0.85 M_{\odot}$) He-burning stars - since the pulsational quantities (i.e. period and amplitude of pulsation) depend on the star structural parameters (mass, luminosity and effective temperature), and are firm and safe observables as well, fully independent of distance and reddening.

On this ground, we planned to construct an exhaustive and homogeneous theoretical framework, both on the pulsational and the evolutionary side, aiming at a sound analysis of observed RR Lyrae stars at various metal contents (see Castellani, Caputo & Castellani 2003, Paper I, for the observational scenario of variables in Galactic globular clusters). Extensive sets of nonlinear convective pulsation models (Di Criscienzo, Marconi & Caputo 2003, Paper III, in preparation) and HB evolutionary tracks (Cassisi, Castellani, Caputo & Castellani 2003, Paper IV, in preparation) are computed using the same input physics. Then, adopting similar bolometric corrections and color-temperature transformations, self-consistent predictions concerning various stellar parameters are derived.

The general procedure is discussed in the present paper, which deals with the results at Z=0.001 and Y=0.24. We selected this metal content as suitable for the analysis of several RR Lyrae rich globular clusters, in particular M3 which is the most RR Lyrae rich cluster in the Galaxy and among the best studied ones. The organization of the paper is as follows: Section 2 presents the pulsation models and gives the relevant relations among the various parameters, while the constraints from stellar evolution theory are discussed in Section 3.

The comparison with available *BVK* photometry of RR Lyrae variables in M3 is presented in Section 4. Discussion and some brief remarks close the paper.

2. Theoretical pulsational scenario

2.1. Pulsation models

The nonlinear convective hydrodynamical code used for pulsation model computations has been already described in a series of papers (see, e.g., Bono & Stellingwerf 1994; Bono et al. 1997a,b) and it will not be discussed further. We wish only to mention that the models adopt recent opacity compilations by Iglesias & Rogers (1996) for temperatures higher than 10,000 K and by Alexander & Ferguson (1994) for lower temperatures. As in previous papers, a mixing length parameter l/H_p=1.5 is adopted in order to close the system of convective and dynamic equations. However, to gain some insight into how the boundaries for instability are dependent on convection (see Caputo et al. 2000), additional models with l/H_p=2.0 are computed, also in view of the values for the mixing length parameter recently used in HB model computations (see Sect. 3).

For the pulsation models with Z=0.001, we adopt two masses (M=0.65 and 0.75$M_\odot$) and three luminosity levels (log$L/L_\odot$=1.51, 1.61, 1.72) in order to explore the dependence on the stellar mass and luminosity. For each given set of entry parameters, the computations are performed by decreasing the effective temperature T_e by steps of 100-200 K. In the following, we refer to the results from the first (bluest) pulsating model to the last (reddest) one. Let us be clearly understood that increasing (decreasing) by 100 K the effective temperature of the bluest (reddest) pulsators yields non-pulsating structures.

Since the adopted nonlinear approach supplies not only the pulsation period, but also the luminosity variation along the whole pulsation cycle, the bolometric light curves are transformed into the observational plane by adopting bolometric corrections and temperature-color transformations provided by Castelli, Gratton & Kurucz (1997a,b, hereafter CGKa,b). In this way, amplitudes and *mean* absolute magnitudes, either intensity-weighted and magnitude-weighted, are derived in the various photometric bands.

Table 1 lists selected results[3] for fundamental (F) pulsators with 0.65$M_\odot$, log$L/L_\odot$=1.61 and l/H_p=1.5. For each given effective temperature, we give the static magnitude, i.e. the value the star would have were it not pulsating, the period P (in days), mean intensity-weighted $< M_i >$ and magnitude-weighted (M_i) magnitudes, and amplitudes A_i. Table 2 has the same meaning, but holds for first-overtone (FO) pulsators.

---

[3] The entire set of models can be obtained upon request to marcella@na.astro.it

As well known since the original Ritter's formulation $P\rho^{1/2}$=Q (ρ is the star density and Q the pulsation constant), the basic physics underlying radial variability suggests that the pulsation period depends on the mass, luminosity and effective temperature of pulsators. Linear interpolation among all our data supplies a refined version of earlier pulsation equations (see, e.g., van Albada & Baker 1971, Bono et al. 1997a), as given by

$$\log P^F = 11.066(\pm 0.002) + 0.832 \log L - 0.650 \log M - 3.363 \log T_e \qquad (1a)$$

$$\log P^{FO} = 10.673(\pm 0.001) + 0.805 \log L - 0.603 \log M - 3.281 \log T_e \qquad (1b)$$

where luminosity L and mass M are in solar units. According to our models, the period of FO pulsators can be "fundamentalized" as $\log P^F - \log P^{FO} \sim 0.13$, on average, or with the more punctual relation $\log P^F$=0.147+1.033$\log P^{FO}$, neglecting the weak dependence on mass and luminosity which plays a significant role only when dealing with double mode pulsators.

The natural outcome of the pulsation equation in the observational plane is the Period-Magnitude-Color (PMC) relation in which the pulsation period, for any given mass, is correlated with the pulsator absolute magnitude and color. Using BV static quantities[4], linear interpolation through the results (see Fig. 1) gives

$$\log P^F = -0.612(\pm 0.002) - 0.340 M_V - 0.663 \log M + 1.307[M_B - M_V] \qquad (2a)$$

$$\log P^{FO} = -0.762(\pm 0.001) - 0.340 M_V - 0.643 \log M + 1.381[M_B - M_V], \qquad (2b)$$

According to the predicted PMC relations, for a sample of RR Lyrae stars at the same distance and with the same reddening, e.g. for variables in a given globular cluster with no differential reddening, one could estimate the mass range spanned by the variables with an uncertainty lower than 2%, once periods and static colors are firmly known. If the cluster distance modulus and reddening are independently determined, then the mass absolute values can be inferred too. Alternatively, once period and color are measured, the relations can be used to get the distance to individual RR Lyrae stars with known mass and reddening.

---

[4] We give here only the predicted relations which are used in comparison with BVK data of M3 RR Lyrae stars. As for the relations in other photometric bands, they can be requested to marcella@na.astro.it.

Let us now consider the quite plain correlation between the absolute magnitude in a given i-band and luminosity, $M_i = -2.5\log L + BC_i$, where the bolometric correction BC_i depends on the star effective temperature, mass and luminosity. Since also the pulsation period is governed [see eqs. (1a) and (1b)] by the effective temperature, mass and luminosity, the absolute magnitude M_i of radial pulsating stars is expected to be a function of mass, luminosity and period. It is obvious that the dependence of M_i on mass, luminosity and period is governed by the dependence of BC_i on the effective temperature.

We show in Fig. 2 (symbols as in Fig. 1) the quite different dependence of visual and near-infrared static absolute magnitudes on the pulsation period. For any given mass and luminosity, an increase of T_e yields shorter periods, while M_V becomes slowly brighter and M_K significantly fainter. On the other hand, if increasing the luminosity at constant mass and effective temperature, the period increases and both M_V and M_K become brighter. In summary, one has a sort of *degeneracy* (see the arrows in the lower panel in Fig. 2) between the luminosity and effective temperature effects on M_K. As a result, for fixed period, M_V depends mainly on luminosity, with a negligible dependence on the mass, whereas M_K shows small but non negligible variations both with luminosity and mass (see also Bono et al. 2001, 2003). According to present models, the predicted period-magnitude relations in the visual (PM_V) and near-infrared bandpass (PM_K) are

$$M_V^F = 5.597(\pm 0.002) + 0.415\log P^F + 0.305\log M - 2.890\log L \qquad (3a)$$

$$M_V^{FO} = 5.478(\pm 0.002) + 0.319\log P^{FO} + 0.253\log M - 2.818\log L \qquad (3b)$$

and

$$M_K^F = -0.182(\pm 0.002) - 2.197\log P^F - 1.447\log M - 0.663\log L \qquad (4a)$$

$$M_K^{FO} = -0.502(\pm 0.002) - 2.272\log P^{FO} - 1.379\log M - 0.659\log L \qquad (4b)$$

The importance of the RR Lyrae near-infrared PM_K relation to get accurate distances to globular clusters has already been discussed by several authors (see Bono et al. 2001 and references therein) and it will not be discussed further. It is enough to mention that near-infrared magnitudes are very little affected by reddening and that adopting for the RR Lyrae stars in a given globular cluster, that is for variables at constant age and metal content, a luminosity dispersion of $\delta \log L \sim \pm 0.06$ and a mass spread[5] of ±3%, yields a dispersion $\delta M_V \sim \pm 0.17$ mag and $\delta M_K \sim \pm 0.05$ mag, at fixed period.

---

[5] Based on current computations, the mass spread of HB models near the RR Lyrae instability strip depends on Z, decreasing with increasing the metal content.

2.2. The instability strip

All the relations described in the previous section originate from the pulsation equation which formally fixes the pulsation period for any given combination of the entry parameters (M, L, T_e). However, it is well known that radial pulsation occurs in a quite well-defined region of the HR diagram, the so-named "instability strip", that depends on the type of pulsation and the intrinsic parameters of pulsators. In simple words, pulsation does not occur for any combination of M, L and T_e. For each given mass and luminosity there is a maximum and minimum effective temperature for the onset of either fundamental and first-overtone pulsation.

As already known, the data in Tables 1 and 2, as those presented in previous papers (see, e.g., Bono, Caputo & Marconi 1995a, Bono et al. 1997a,b, Caputo et al. 2000, Bono et al. 2002 and references therein) show that, for fixed mass and luminosity, FO pulsators are generally bluer than F pulsators, in full agreement with the observed behavior of *c*-type and *ab*-type RR Lyrae stars. This yields that the first-overtone blue edge (FOBE) and the fundamental red edge (FRE) can be taken as limits of the whole instability strip. Moreover, the models show that the fundamental pulsation blue edge (FBE) is generally bluer than the first-overtone red edge (FORE), suggesting that both the pulsation modes can be stable in a middle region of the instability region. Such a result supports the hypothesis that the transition between *ab* and *c* type RR Lyrae stars may occur along different transitions (FBE or FORE), as well as that a hysteresis mechanism, as earlier suggested by van Albada & Baker (1973), could explain the Oosterhoff dichotomy (see, e.g., Bono et al. 1995a, Bono et al. 1997a for details).

Given the steps of 100 K in our computations, we adopt as edges of the pulsation region the effective temperature of the bluest FO model and of the reddest F model, increased and decreased by 50K, respectively. Then, linear interpolation to all the data with Z=0.001 and l/H_p=1.5 gives the following relations

$$\log T_e^{FOBE} = 3.970(\pm 0.004) - 0.057 \log L + 0.094 \log M \tag{5}$$

$$\log T_e^{FRE} = 3.957(\pm 0.007) - 0.102 \log L + 0.073 \log M \tag{6}$$

where the uncertainties include the intrinsic uncertainty of ±50K on the FOBE and FRE temperatures.

Before proceeding, it is worth mentioning that a further source of uncertainty on the pulsation limits is due to the efficiency of convection in the star external layers. As the depth of convection increases from high to low effective temperature, and the effect of convection is to quench pulsation, we expect that varying the value of the mixing length parameter will modify the red edge of the instability strip by a larger amount with respect to the blue edge. Model computations made with l/H_p=2.0 show that, at constant mass and luminosity, the FOBE temperature decreases by $\sim$ 100 K, whereas those at FBE and FRE increase by $\sim$ 100 K and $\sim$ 300 K, respectively. As a consequence, at l/H_p=2.0 the zero-point in eq. (5) and eq. (6) varies by -0.006 and $+0.020$, respectively. Note that the knowledge of FOBE and FRE effective temperatures is basic to select variable and non variable stars in synthetic HB populations (see Sect. 3.2)

For comparison with observed RR Lyrae stars, of particular interest (see Caputo 1997; Caputo et al. 2000) is the location of the pulsation theoretical edges in the magnitude-period and color-period diagrams. From present models at Z=0.001 and l/H_p=1.5, and adopting CGKa,b atmosphere models, we derive

$$M_V^{FOBE} = -1.193(\pm 0.034) - 2.230 \log M - 2.536 \log P^{FO} \quad (7)$$

$$M_V^{FRE} = 0.119(\pm 0.040) - 1.883 \log M - 1.962 \log P^{F} \quad (8)$$

and

$$[M_B - M_V]^{FOBE} = 0.25(\pm 0.02) - 0.10 \log M + 0.10 \log P^{FO} \quad (9)$$

$$[M_B - M_V]^{FRE} = 0.48(\pm 0.03) - 0.06 \log M + 0.27 \log P^{F} \quad (10)$$

where the uncertainties include the intrinsic ±50 K uncertainty on the FOBE and FRE temperatures. As a consequence of the above mentioned effects of a larger mixing-length parameter on the FOBE and FRE effective temperatures, adopting l/H_p=2.0 the zero-point in eq. (7) and eq. (8) varies by $\sim +0.05$ mag and ~ -0.14 mag, respectively, while in eq. (9) and eq. (10) by $\sim +0.02$ mag and ~ -0.06 mag, respectively.

2.3. Pulsation amplitudes

We have already mentioned that the non-linear approach supplies important clues on a further observable: the pulsation amplitude. A glance at the data in Table 1 and Table 2 (see also Bono et al. 1997a) shows that, for fixed mass and luminosity, there is a direct correlation between fundamental amplitude and effective temperature: the amplitude increases when moving from the red to the blue limit for fundamental pulsation, that is as the period decreases. As for FO pulsators, they show a characteristic “bell” shaped distribution, with the maximum amplitude attained in the middle of the first-overtone region. As a whole, these theoretical features appear consistent with observed RR Lyrae period-amplitude diagrams, usually named "Bailey diagrams" after their inventor (Bailey 1899, 1902).

Taking advantage of the quite linear correlation between fundamental amplitude and period (logarithmic scale), we show in the left panel of Fig. 3 the A_V-log$P$ distribution of F pulsators at l/H_p=1.5 and different mass and luminosity (symbols as in Fig. 1). One has that, for fixed period, the amplitude decreases as the luminosity decreases or, by a rather small amount, as the mass increases. As a whole, we show in the right panel in Fig. 3 that all the results with l/H_p=1.5 (filled circles) can be approximated with the linear relation (solid line)

$$\log P^{F*} = \log P^F + 0.385M_V + 0.299\log M = 0.132(\pm 0.02) - 0.189A_V \tag{11}$$

However, we wish to remark that the fundamental pulsation amplitude is not "*governed*" by the absolute value of the effective temperature, but it depends on the "*relative*" location of the pulsator with respect to the red limit (where vanishing amplitudes are attained) and blue limit (where the amplitude reaches it maximum value) of fundamental pulsation (see also Bono et al. 1997a). As a matter of example, the visual amplitude of the $0.65M_\odot$ pulsator with T_e=6500 K increases from A_V=0.77 to 1.05 mag as the luminosity increases from log$L/L_\odot$=1.51 to 1.72. It follows that the above described effects of a larger mixing-length parameter on the effective temperature of the fundamental pulsation limits will modify both the zero-point and the slope of the predicted Period-Magnitude-Amplitude (PMA) relation. As a fact, the right panel in Fig. 3 shows that the results with l/H_p=2.0 (open circles) can be approximated as (dotted line)

$$\log P^{F*} = \log P^F + 0.385M_V + 0.349\log M = 0.024(\pm 0.02) - 0.142A_V \tag{12}$$

Closing this section on the pulsation amplitude, we present in the left panel in Fig. 4 the relation between visual amplitude A_V and static BV color for F pulsators with l/H_p=1.5 (symbols as in Fig. 1). One derives that, at least in the explored range of mass and luminosity, all the results can be approximated with a common Color-Amplitude (CA_{BV}) relation, as given by (see the solid line in the right panel)

$$M_B - M_V = 0.49(\pm 0.02) - 0.137A_V \tag{13}$$

However, for the reasons above discussed, also the CA_{BV} relation turns out to depend on the adopted mixing-length parameter, becoming

$$M_B - M_V = 0.42(\pm 0.02) - 0.113 A_V \tag{14}$$

at l/H_p=2.0 (see the dotted line in the right panel).

According to the predicted CA_{BV} relation, the intrinsic BV color of individual pulsators can be estimated within ±0.02 mag, which means a similar accuracy in the knowledge of the reddening $E(B-V)$ and a determination of the visual extinction correction A(V) within $\sim \pm$ 0.06 mag. This might be of particular relevance in the case of RR Lyrae variables in globular clusters, or stellar fields, with highly differential reddening.

2.4. Static and mean magnitudes

All the relations presented so far, although involving observable quantities such as magnitude and color, cannot be straightaway applied to observed RR Lyrae variables because they hold for *static* values whereas empirical measurements refer to quantities averaged over the pulsation cycle.

From the data listed in Table 1 one finds that the synthetic mean magnitudes (M_i) of fundamental pulsators, as derived averaging the magnitude over the cycle, are fainter than the corresponding static values with a discrepancy increasing as the pulsation amplitude increases. The key element governing such a behavior is the overall morphology of the light curve in the sense that the difference between static and mean magnitudes increases from symmetric (low amplitude) to asymmetric (high amplitude) light curves, namely moving from the red to the blue fundamental edge (see also Bono, Caputo, Stellingwerf 1995b). Since at fixed effective temperature the amplitude decreases from blue to visual to infrared, the difference between static and mean values for K magnitudes is almost negligible, whereas (M_B), (M_V) and (M_I) differ from the corresponding static values up to $\sim$ 0.18 mag, $\sim$ 0.14 mag, and $\sim$ 0.08 mag, respectively, at A_V=1.6 mag. As for FO pulsators (data in Table 2), the discrepancy is less pronounced, given their low-amplitude and quite symmetric light curves. Note that present synthetic magnitudes confirm previous BVK results inferred by Bono et al. (1995b) from a preliminary set of pulsating models with Z=0.001, but adopting Y=0.30, older opacity tables (Cox & Tabor 1976) and Kurucz (1992) stellar atmosphere models.

Concerning the intensity-averaged magnitudes $< M_i >$, data in Table 1 and Table 2 confirm that they are quite close to the static values, except for models with very large amplitude.

In Fig. 5 we show the synthetic visual magnitudes for F and FO pulsators, by plotting the discrepancy between static and mean values, as well as the internal difference between the two means, as a function of the visual amplitude A_V. It is quite relevant to notice that the predicted differences $(M_V)- < M_V >$, as well as the corresponding rather insignificant amounts inferred from Table 1 and Table 2 for the K-band, are in close agreement with observed differences $(V)- < V >$ and $(K)- < K >$, as reported in previous studies on RR Lyrae stars (e.g. Fernley 1993).

As for the mean colors $m_i - m_j$ which are usually estimated using either $(m_i) - (m_j)$ or $< m_i > - < m_j >$, since most of empirical work on RR Lyrae stars refers to B and V magnitude, we show in Fig. 6 the predicted discrepancy between static and mean $B - V$ color, as well as the difference between the two means $(M_B - M_V)$ and $< M_B > - < M_V >$. At variance with the behavior shown in Fig. 5, one has that the $(M_B - M_V)$ color is redder, whereas $< M_B > - < M_V >$ is bluer, than the static color. The evidence for a positive difference between predicted $(M_B - M_V)$ and $< M_B > - < M_V >$, with an amount that increases with A_V, agrees with quite well settled observed trends (see, e.g. Liu & Janes 1990; Storm, Carney & Beck 1991; Carney et al. 1992, Caputo et al. 1999).

According to the data presented in Fig. 5 and Fig. 6, mean magnitudes and colors can be corrected for the amplitude effect to get static values (see also Bono et al. 1995b). However, given the different behavior of $M_i - (M_i)$ and $M_i- < M_i >$ with the amplitude, we find that static BV magnitudes can be directly estimated when both the mean quantities are measured. In particular, either for F and FO pulsators, we derive that static BV values (see Table 2 for the other bands) can be approximated as

$$M_V = -0.345(M_V) + 1.345 < M_V > \tag{15}$$

$$M_B - M_V = 0.488[(M_B - M_V)] + 0.497[< M_B > - < M_V >] \tag{16}$$

with an intrinsic uncertainty of ±0.01 mag.

3. The evolutionary connection

At the beginning of this paper we mentioned that the “theoretical route” to the calibration of the M_V(RR) versus [Fe/H] relation, as inferred by HB evolutionary models, suggests brighter magnitudes than empirical estimates, at fixed [Fe/H]. Unfortunately, even the amount of this over-luminosity is still matter of controversy.

For the sake of the following discussion, let us briefly summarize the basic ingredients which are needed for a reliable "theoretical route":

1. Trustworthy HB models computed with the most recent updating of the relevant physics.
2. Synthetic HB simulations (SHB) in order to estimate the evolutionary effects and the role of different HB populations.
3. Realistic bolometric corrections and color-temperature transformations.
4. Appropriate scaling between the metallicity Z and the iron-to-hydrogen content [Fe/H].

Such a "shopping list" should help the common reader to understand the main reasons for the rather different theoretical predictions on the M_V(RR)-[Fe/H] relation, as presented in the recent literature (see Caputo et al. 2000 and references therein).

It is known that, due to somehow different input physics, current updated HB models still provide slightly different luminosity values (see, e.g., Castellani 2003). Moreover, different bolometric corrections, as well as different assumptions concerning the value of the overabundance of α-elements with respect to iron, are used by the various researchers. We add that sometimes, in order to account for the luminosity of actual (evolved) pulsators, the zero age horizontal branch (ZAHB) luminosity at the RR Lyrae instability strip is artificially increased, by a fixed quantity or as a function of metallicity, instead of making use of SHB results.

Within such a complex scenario, it is of primary importance to carefully investigate into current uncertainties of HB models. This will be done in the following section where the HB models at Z=0.001 ([α/Fe=0]) computed by Cassisi et al. (2003, in preparation, hereafter C03), are compared with VDB results.

3.1. The zero age horizontal branch

According to a very common procedure, ZAHB stars are investigated starting from stellar structures with the same mass of the He core and the same chemical composition of the stellar envelope as in the RG progenitor at the He ignition, but with an increased abundance of Carbon in the He core by about 5% by mass as a result of the flash. The mass of the H-rich envelope and, thus, the total mass of the model are regarded as a free parameter governed by the unknown amount of mass loss. A reliable ZAHB model is eventually obtained by evolving such an initial structure for about 1 Myr to allow equilibrium of CNO elements in the H burning shell (see, e.g., Caputo, Castellani & Wood 1978, Caputo, Castellani & Tornambe' 1978, Castellani, Chieffi & Pulone 1991).

The C03 horizontal branch models used in this paper implement previous calculations presented by Cassisi et al. (1999) and Caputo & Cassisi (2002) and will not discussed here. Of importance is that both C03 and VDB models adopt quite similar values for the mixing length parameter (l/H_p=2.0 and 1.9, respectively), no helium and heavy element diffusion, and can be taken as representative of the range in *absolute magnitude* spanned by recent HB evolutionary calculations with updated input physics.

Figure 7 shows the mass and luminosity of ZAHB models near the RR Lyrae instability strip plotted as a function of the effective temperature. As for the VDB models, note that they have the same *overall* metallicity Z=0.001, although referring to different chemical mixtures ([α/Fe]=0, [Fe/H]=$-$1.31 and [α/Fe]=0.3, [Fe/H]=$-$1.54).

From the comparison of models at fixed effective temperature, one finds evidence for three main points:

1. C03 models are brighter by $\delta\log L \sim 0.01$ dex;
2. C03 models are more massive by $\sim 0.02M_\odot$;
3. increasing [α/Fe] up to 0.3, which is the mean value estimated for globular cluster stars with [Fe/H]< -0.6 (see Carney 1996), leaves quite unvaried the value of mass and luminosity. In other words, at least in the range of RR Lyrae effective temperature and with no significantly large [α/Fe] values, either the mass and the luminosity of pulsators are expected to depend on the overall metallicity Z, quite independently of the internal ratio between α and heavy elements (see also Salaris, Chieffi & Straniero 1993).

As a first step, in order to gain some insight into the predicted distribution of ZAHB pulsators, we evaluate for each model the predicted FOBE and FRE, by inserting the mass and luminosity of the model into eq. (5) and eq. (6), respectively, but with a modified zero-point accounting for the mixing length parameter adopted in the quoted evolutionary computations. In this way, synthetic ZAHB pulsators are easily identified with the models for which holds FOBE $\geq \log T_e \geq$ FRE.

As shown in Fig. 8 for C03 computations, one derives that the mass of predicted ZAHB pulsators with Z=0.001 should vary from ~ 0.65 (FOBE) to $\sim 0.67M_\odot$ (FRE), and accordingly the luminosity increases from log$L/L_\odot$=1.67 to 1.69. As for VDB ZAHB models, we get mass in the range of $\sim$ 0.63 to 0.65$M_\odot$ and luminosity from log$L/L_\odot$=1.66 to 1.68. It is worth mentioning that, since mass and luminosity vary in the same direction, both sets of computations turn out to agree each other as the effective temperature and the period of ZAHB pulsators are concerned. We estimate that the effective temperature of ZAHB pulsators varies from log$T_e \sim 3.85$ (FOBE) to ~ 3.79 (FRE), while the predicted periods at the edges of the instability strip are logP^{FO}(FOBE)~ -0.50 and logP^F(FRE)~ -0.15, that are in reasonable agreement with the observed color and period distributions of RR Lyrae stars in globular clusters with well populated HB (see Paper I).

3.2. Post ZAHB evolution and synthetic HB

Since the first pioneering work by Rood (1973), the major way of interpreting the properties of observed HB and RR Lyrae stars deals with synthetic horizontal branches (SHB) constructed on the basis of HB evolutionary tracks. The literature of the last three decades is rather abundant (readers are referred to Ferraro et al. (1999), Demarque et al. (2000) and references therein). However, until now we have no knowledge of synthetic simulations as based on either recent up-to-date HB models *and* pulsation theory (i.e. nonlinear, convective models). For this reason, an atlas of SHBs with various metal content has been planned (Paper IV) with the purpose to determine a series of parameters (HB morphology, RR Lyrae luminosity, period distribution, etc) which are needed to realistic discussion of observed HB and RR Lyrae stars in globular clusters.

Figures 9 and 10 illustrate the results of two of these SHBs at Z=0.001: specifically, those adopting a total number of HB stars N(HB)=400, a mean mass of HB stars M(HB)=0.65 and 0.69$M_\odot$, and a mass dispersion factor by 0.02$M_\odot$ (see Demarque et al. 2000). Following the procedure described for ZAHB models, synthetic HB stars hotter (cooler) than their predicted FOBE (FRE) are taken as blue (red) stable stars, while those with FOBE$\geq$ log$T_e \geq$ FRE are identified as pulsating structures. In this way, the predicted numbers of blue (B), variable (V) and red (R) stars are derived, leading to the (B-R)/(B+V+R) ratio (Lee 1990) labelled in the two panels. In the figures, the solid line is the ZAHB, while the dashed vertical ones depict the predicted edges of the RR Lyrae instability strip.

Besides the well known correlation between the average mass M(HB) and the HB morphology (lower is the mean mass of HB stars bluer their color distribution, everything else being constant), we should mark three points:

1. synthetic pulsators are brighter and, on average, slightly more massive than ZAHB ones. Note that the brightest stars populating the RR Lyrae instability strip are also the less massive ones;

2. the lower envelope of the evolved star luminosities is slightly brighter than the ZAHB luminosity level (see also Ferraro et al. 1999). Note that this may depend on the above definition of "ZAHB" (Sect. 3.1.);

3. the average mass of the variable stars is quite constant, $< M(RR) >=0.67\pm0.02M_\odot$, in the quoted range of M(HB) and (B-R)/(B+V+R) ratio. We show in Table 4 that, as long as the fraction of variables is statistically significant [V/(B+V+R)$\geq$0.20], the above value for the pulsator average mass holds for (B-R)/(B+V+R) ratio in the range of $\sim$+0.55 to ~ -0.45, whereas for bluer or redder HB distributions the SHB results suggest $< M(RR) >=0.66\pm0.02M_\odot$ and $0.68\pm0.02M_\odot$, respectively. With small numbers of variables, i.e. very blue or very red HB distributions, no statistically reliable information on the average mass $< M(RR) >$ can be derived.

Let us now investigate the distribution of the synthetic HB pulsators, namely of the evolved stellar structures satisfying the condition FOBE $\geq$ logT_e $\geq$ FRE, in the M_V-log$P$ plane. We present the case at M(HB)=0.67$M_\odot$ (HB index $\sim$ 0.10, as observed in M3), but quite similar results are obtained with M(HB)=0.65 and 0.69$M_\odot$. As already mentioned, we adopt CGKa,b bolometric corrections.

The left panel in Fig. 11 deals with the short-period side of synthetic first overtone pulsators [periods from eq. (1b)]. The solid line is the resulting FOBE of the synthetic distribution (see the labelled relation), while the dashed lines depict its intrinsic dispersion [see eq. (5)] of ± 0.034 mag. In the right panel, which refers to the long-period side of fundamental periods [periods from eq. (1a)], the solid and dashed lines depict the predicted FRE (see labelled relation) and its intrinsic uncertainty by ± 0.04 mag [see eq. (6)], respectively. The horizontal line drawn in the two panels depicts the lower envelope magnitude $M_{V,le}$=0.55 mag of the synthetic pulsator distribution.

A question that should be soon asked is "how far the above predictions on the FOBE and FRE of evolved pulsators are model-dependent?". Bearing in mind the main differences between C03 and VDB models (see Fig. 7), we have generated "VDB-like" synthetic populations by simply decreasing mass and luminosity of our HB models by 0.02$M_\odot$ and 0.01 dex, respectively, and maintaining CGKa,b bolometric corrections. As a result, we get that either FOBE and FRE magnitudes should be increased by $\sim$ 0.03 mag, at fixed period, as well as that the absolute magnitude of the lower envelope is $M_{V,le}$=0.58 mag.

4. The RR Lyrae population in M3

We are now in the position to undertake an exhaustive comparison between the pulsational predictions presented in the previous sections and the observed properties of RR Lyrae stars in M3. Taking advantage of the extensive set of BV photometric data provided by Corwin & Carney (2001), we select[6] a fiducial sample of variables with quite well-measured periods, mean magnitudes and amplitudes. In the following discussion, we will adopt $E(B-V)$=0.

Figure 12 shows the variables (different pulsation modes follow Corwin & Carney (2001) classification) plotted in the color-magnitude diagram, according to magnitude-averaged (upper panel) and intensity-averaged (lower panel) quantities. As a matter of reference, we draw a line at V=15.8 mag. At first sight, the *ab*-type magnitude plotted in the upper panel are on average fainter than in the lower panel. Moreover, the magnitude-averaged color of the bluest *ab*-type variables, is evidently redder than the intensity-averaged one. As an example, V77 shows $(B-V)$= 0.279 mag and $<B>-<V>$=0.223 mag.

And indeed, we show in Fig. 13 that, with the only exception of variable V82 (filled triangle), the behavior of the measured difference between the empirical mean quantities follows the predictions presented in Fig. 5 and Fig. 6 faithfully. On this ground, eq. (15) and eq. (16) are used to get static magnitudes and colors, with an error of ± 0.01 mag, giving us the opportunity to compare the predictions presented in the previous sections with observed data.

Let us firstly consider the predicted relations which are independent, or slightly dependent, of mass and luminosity.

a) The Color-Amplitude relation

Figure 14 shows the visual amplitude of *ab*-type variables in M3 as a function of the static $B-V$ color, in comparison with the predicted CA_{BV} relations at l/H_p=1.5 (solid line) and 2.0 (dotted line). Bearing in mind the intrinsic dispersion (± 0.02 mag in color, at fixed amplitude) of the predicted relations, and allowing for photometric errors, the agreement between theory and observations is reasonably good, disclosing also a quite interesting feature: at the larger amplitudes, the observed data are not allowing a firm choice between the two adopted values of the mixing-length parameter, but moving towards redder colors the measured amplitudes are clearly pointing to l/H_p=2.0.

b) The Color-Period diagram

---

[6] Variables with Blashko effect, blend or less precise periods are excluded.

Figure 15 shows the RR Lyrae stars in M3 (symbols as in Fig. 12) plotted in the $B-V$ versus period diagram, in comparison with the predicted FOBE [eq. (9)] and FRE [eq. (10)] at l/H_p=1.5 (solid line) and 2.0 (dotted line). As for the mass of the variables, we adopt the value $<M(RR)>$=0.67±0.02$M_\odot$ suggested by the SHB results presented in Fig. 9, bearing in mind that the color of the predicted edges depends very little on the mass. Taking into account the intrinsic uncertainty (± 0.02 mag) of the predicted color at fixed period, the data plotted in Fig. 15 show that the reddest *ab*-type variables closely match the predicted FRE with l/H_p=2.0, excluding the case l/H_p=1.5, unless a *negative* reddening is adopted.

Concerning the bluest *c*-type variables, excluding V177 and V178, they are in a marginal agreement with the theoretical FOBE with l/H_p=1.5, whereas the case l/H_p=2.0 appears significantly too red. As for the location of V177 and V178, one has three possible choices, provided that the measured color is correct: 1) the variables are not *bona fide* FO pulsators (second overtones ?); 2) the variables are dramatically more massive ($\sim$ 50%) than the bulk of M3 variables [see eq. (9)]; 3) the actual FOBE is bluer than predicted with l/H_p=1.5. As for the last case, we estimate that adopting a mixing-length parameter $l/H_p \sim 1.1$ will move blueward the FOBE (see Caputo et al. 2000) by the needed shift $\sim$ 0.02 mag, at fixed period.

Let us now proceed with predicted relations involving mass and luminosity of the variables, beginning with those which are independent of the edges of the instability strip, and then of the adopted mixing-length parameter.

c) Period-Magnitude-Color relation

According to eq. (2a) and eq. (2b), one may constrain the mass of RR Lyrae stars for each given assumption on the distance modulus DM or, alternatively, one can derive the distance modulus for each given value of the mass.

Adopting two alternative values for the cluster distance modulus, DM=14.9 and 15.2 mag, taken as roughly representative of the range of current estimates (see Saad & Lee 2001), we show in Fig. 16 the reduced fundamentalized period ($\log P^F$+0.34M_V) of RR Lyrae stars in M3 (symbols as in Fig. 12) as a function of the static $B-V$ color. As a whole, the data reasonably follow the predicted slope at constant mass (solid line), even though the observations would suggest a slope of 1.05 which is less than the predicted one. It seems of interest to note that previous simulations (Rood 1990) do show that observational color errors do make the observed slope less than the theoretical one.

According to the predicted relations, increasing DM from 14.9 to 15.2 mag, the average mass of RR Lyrae stars increases from $\sim$ 0.54 to 0.77$M_\odot$, largely encompassing the value $< M(RR) >$=0.67±0.02$M_\odot$ suggested by the SHB results presented in Fig. 9. As a fact, if the *evolutionary* mass is adopted, then the resulting distance modulus is $DM(PMC)$=15.09±0.08 mag.

As a fact, if the *evolutionary* mass is adopted, then the resulting distance modulus is $DM(PMC)$=15.09±0.08 mag.

Interesting enough, inspection of Fig. 16 shows that the reduced period of V177 and V178 is longer with respect to the general behavior of M3 *c*-type variables. According to eq. (2b), this difference should suggest that the mass of these variables is smaller ($\sim$ 20%) than the remaining *c*-type stars, at variance with the mass variation we needed in Fig. 15 to bring their color in agreement with the predicted FOBE. On the other hand, if a decrease of the mixing-length parameter can be invoked in Fig. 15 to move blueward the predicted FOBE, this is without significance for what the PMC relation is concerned. Furthermore, we could also exclude that these variables are second-overtone pulsators since in such a case one expects shorter periods than first-overtone pulsation, at fixed color (i.e. T_e). In conclusion, the pulsation models would suggest that the measured color of V177 and V178 should be increased by $\sim$ 0.03 mag, as required by both the FOBE location and the PMC relation.

d) Near-infrared period-magnitude relation

Proceeding in our analysis, we compare measured K magnitudes of RR Lyrae stars in M3 with the predicted near-infrared period-magnitude relation. Using Longmore at al. (1990) near-infrared photometry and fundamentalized periods, we show in Fig. 17 that the data arrange quite well along the predicted slope at constant mass and luminosity (solid line). Since the predicted M_K magnitude is slightly dependent on the intrinsic luminosity (see lower panel in Fig. 2), we adopt log$L$=1.75±0.15 as a quite safe luminosity range for RR Lyrae with Z=0.001. Then, taking again $< M(RR) >$=0.67±0.02$M_\odot$, we derive $DM(PM_K)$=15.08±0.06 which is very close to the PMC result.

e) Period-magnitude-amplitude relation

As a further independent method to estimate the distance modulus, let us consider the period-magnitude-amplitude (PMA) of fundamental pulsators. Note that now one has different results, depending on the mixing-length parameter [see eq. (13) and eq. (14)], for each given mass. Adopting again $< M(RR) >$=0.67±0.02$M_\odot$, we shown in Fig. 18 that fitting observed data to the predicted PMA relations with l/H_p=1.5 (left panel) and l/H_p=2.0 (right panel) yields $DM(PMA)$=14.98±0.08 mag and 15.09±0.07 mag, respectively.

f) Edges of the instability strip

Figure 19 finally illustrates the comparison between the observed distribution of RR Lyrae stars in the V-log$P$ plane and the predicted edges of the instability strip, as inferred by SHB simulations with l/H_p=2.0 (see Fig. 11). One has that a nice agreement between predictions and observations is attained adopting DM=15.04 mag, even though the period of a couple of c-type variables turns out be slightly shorter than the predicted limit. On the other hand, if the distance modulus is slightly decreased (DM=15.0 mag) in order to leave no c-type variables in the hot stable region, then a few ab-type variables would have slightly longer period than the predicted FRE.

As far a decrease of the adopted mixing-length parameter is concerned, one has to consider that at l/H_p=1.5 the predicted edges becomes brighter by 0.05 mag (FOBE) and fainter than 0.14 mag (FRE), at constant period. As a consequence, a distance modulus DM=15.05 mag is the right value to fit the observed distribution of c-type variables, whereas ab-type variables would require DM=14.90 mag.

We summarize in Table 4 the distance moduli inferred by the different pulsational methods discussed so far. One can conclude that the assumption l/H_p=1.5 yields rather discordant results, while a quite close agreement among the various approaches is reached with l/H_p=2.0. However, we have shown in Fig. 15 that adopting such a large value of the mixing-length parameter the predicted FRE fully accounts for the observed colors of ab-type variables, whereas the predicted FOBE is too red in comparison with the observed colors of c-type variables. On this issue, it seems interesting to mention a recent paper by Bono, Castellani & Marconi (2002) dealing with the comparison of observed light curves of bump Cepheids in the Large Magellanic Cloud with theoretical predictions. In that paper it is shown that for short-period variables a nice agreement is attained with l/H_p=1.5, whereas long-period Cepheids, which are located close to the red edge of the pulsation region, require a higher value (l/H_p=1.8), suggesting that the mixing-length parameter increases when the effective temperature decreases, and the convective layer becomes thicker.

Eventually, we adopt that the mixing-length parameter increases from FOBE (l/H_p=1.5) to FRE (l/H_p=2.0). As a result, we derive that the *pulsational* distance modulus of M3, as given by the weighted mean over the data listed in Table 4, is DM=15.07±0.05 mag, at least adopting RR Lyrae masses from C03 HB models and CGKa,b bolometric corrections.

5. Discussion and final remarks

In the previous section we have presented evidence that theoretical relations based on pulsating models with $Z = 0.001$, collated with information on the average mass of RR Lyrae stars inferred by SHB computations, provide a *pulsational* route to accurate distance determinations for globular clusters with well populated horizontal branch. In particular, adopting $< M(RR) >=0.67\pm0.02M_\odot$ from SHB calculations based on C03 HB models, we derived predictions for fundamental (F) or first-overtone (FO) RR Lyrae stars in globular clusters with (B-R)/(B+V+R) ratio from $\sim$+0.55 to ~ -0.45.

The comparison with RR Lyrae stars in M3 (BV data by Corwin & Carney 2001, K data by Longmore et al. 1990) discloses that the pulsating models support the large value of the mixing-length parameter (l/H_p=1.9-2.0) adopted in updated evolutionary computations to fit observed Red Giant Branches, even though they suggest that the value of such a parameter may increase from the blue to the red edge of the instability region. On this basis, adopting CGKa,b bolometric corrections and color-transformations, we eventually get a *pulsational* distance modulus DM(M3)=15.07±0.05 mag, as given by the weighted mean over the results provided by the different approaches (see Table 4).

In order to compare this result with the classical *evolutionary route*, let us go back to Fig. 10. There, we have shown that the lower envelope of the absolute magnitudes of synthetic pulsators based on C03 HB models is at $M_{V,le}$=0.55 mag. On the other hand, we show in Fig. 20 that the actual lower envelope for the M3 variables is V=15.7 mag (solid line), thus providing an *evolutionary* distance modulus DM=15.15 mag which is 0.08±0.05 mag longer than the *pulsational* value.

Before discussing such a small but equally disturbing discrepancy between the pulsational and evolutionary approach, let us mark that it *does not depend on the adopted HB models, nor on the adopted bolometric correction.* In fact, were the VDB models used, but maintaining CGKa,b bolometric corrections, then the average mass of RR Lyrae pulsators would be $0.65\pm0.02M_\odot$ (point 2 in Sect. 3.1), and consequently the distance modulus based on PMC, PMA and PM_K relations should be decreased by $\sim$ 0.02 mag, on average. On the other hand, the predicted FOBE and FRE magnitudes, at fixed period, increases by 0.03 mag (see Fig. 11). As a consequence, the pulsational distance modulus of M3 becomes DM=15.05±0.05 mag. Since the lower envelope of the VDB-like pulsators is at $M_{V,le}$=0.58 mag (see Fig. 11), one derives again that the pulsational approach yields a distance modulus larger by 0.07±0.05 mag with respect to the evolutionary predictions.

As for the effects of different bolometric corrections, it is worth mentioning that there is a significant difference between CGKa,b values and those adopted in VDB models, in the sense that the former give absolute magnitudes brighter by $\sim$ 0.05-0.06 mag, at fixed luminosity and effective temperature. However, such a difference obviously modifies the absolute magnitudes, and then the derived distance modulus, but leaves unvaried relative values, mainly the above discrepancy between pulsational and evolutionary distance moduli.

In summary, the distance modulus of M3, as based on pulsational models and mass constrained by stellar evolution theory, ranges from 15.00 mag (VDB computations and bolometric corrections) to 15.05 mag (VDB computations and CGKa,b bolometric corrections) to 15.07 mag (C03 computations and CGKa,b bolometric corrections), all with a total error of ± 0.05 mag. It follows that recent HB computations with updated physics do yield consistent results, *provided that similar bolometric corrections are used.* Conversely, current uncertainty on the *BC* scale appears still too large, requiring some firm solutions.

Independently of the adopted *BC* correction, the pulsational approach would suggest that current updated HB models are over-luminous by 0.08±0.05 mag. However, a clear way to reduce the HB luminosity is offered by the diffusion of helium and metals. As shown by Cassisi et al. (1999), if element diffusion is properly taken into account, then the luminosity of HB models at the RR Lyrae gap decreases by 0.03-0.04 mag, reducing the discrepancy between pulsational and evolutionary distances to $\sim 1\sigma$.

6. Acknowledgments

We thank our referee, B. Rood, for very useful comments and suggestions. Financial support for this work was provided by MIUR-Cofin 2000, under the scientific project “Stellar Observables of Cosmological Relevance”. Model computations made use of resources granted by the “Consorzio di Ricerca del Gran Sasso”, according to Project 6 “Calcolo Evoluto e sue Applicazioni (RSV6) - Cluster C11/B”.

REFERENCES

Alexander, D. R. & Ferguson J.W. 1994, ApJ, 437, 879

Bailey, S. I. 1899, ApJ, 10, 261

Bailey, S. I. 1902, Harv. Coll. Observ. Annals, 38, N.1

Bono, G., Caputo, F. & Marconi, M. 1995a, AJ, 110, 2365

Bono, G., Caputo, F. & Stellingwerf, R. F. 1995b, ApJS, 99, 263

Bono, G., Caputo, F., Castellani, V., Marconi, M. 1997a, A&AS, 121, 327

Bono, G., Caputo, F.,Castellani, V., Marconi, M, Storm, J. 2001, MNRAS, 326, 1183

Bono, G., Caputo, F.,Castellani, V., Marconi, M, Storm, J. 2002, MNRAS, 332,78

Bono, G., Caputo, F.,Castellani, V., Marconi, M, Storm, J., Degl'Innocenti, S. 2003, MNRAS, in press (astro-ph/0306142)

Bono, G., Caputo, F., Cassisi, S., Incerpi, R., Marconi, M. 1997b, ApJ, 483, 811

Bono, G., Castellani, V., Marconi, M. 2002, ApJ, 565, 83

Bono, G. & Stellingwerf, R. F. 1994, ApJ S. S., 193, 233

Cacciari, C., 1999, ASP 167, 140

Caputo, F. 1997, MNRAS, 284, 994

Caputo, F., Castellani, V, Marconi, M., Ripepi, V. 1999, MNRAS, 306, 815

Caputo, F. & Cassisi, S. 2002, MNRAS, 333, 825

Caputo, F., Castellani, V., Marconi, M., Ripepi, V. 2000, MNRAS, 316, 819

Caputo, F., Castellani, V., Tornambè, A. 1978, A&A, 67, 107

Caputo, F., Castellani, V., Wood, P. R. 1978, MNRAS, 184, 377

Carney, B. W., Storm, J., Trammel, S. R., Jones, R. V. 1992, PASP, 104, 44

Carney, B. W. 1996, PASP, 108, 900

Cassisi, S., Castellani, V., Degl'Innocenti, S., Salaris, M., Weiss, A. 1999, A&AS, 143, 103

Castellani, V. 2003, in "New Horizons in Globular Cluster Astronomy", in press

Castellani, M., Caputo, F., Castellani, V. 2003, A&A, accepted (Paper I)

Castellani, V., Chieffi, A., Pulone, L. 1991, ApJS, 76, 911

Castelli, F., Gratton, R. G., Kurucz, R. L. 1997a, A&A, 318, 841 (CGKa)

Castelli, F., Gratton, R. G., Kurucz, R. L. 1997b, A&A, 324, 432 (CGKb)

Corwin, T. M. & Carney, B. W. 2001, AJ, 122, 3183

Cox, A. N. & Tabor, J.E 1976, ApJS, 31, 271

Demarque, P., Zinn, R., Lee, Y.W., Yi S. 2000, AJ, 119, 1398

Fernley, J. 1993, A&A, 268, 591

Fernley, J., Skillen, I., Carney, B. W., Cacciari, C., Janes, K. 1998, MNRAS, 293, 61

Ferraro, F. R., Messineo, M., Fusi Pecci F., de Palo, M. A., Straniero, O., Chieffi, A., Limongi, M. 1999, AJ, 118, 1738

Groenewegen, M. A. T. & Salaris, M. 1999, A&A, 348, 33

Iglesias, C. A. & Rogers, F. J. 1996, ApJ, 464, 943

Kurucz, R. L., 1992, in IAU Symp. 149, 225

Lee, Y. -W. 1990, ApJ, 363, 159

Liu T. & Janes K.A., 1990, ApJ, 354, 273

Longmore, A.J., Dixon, R., Skillen, I., Jameson, R.F., Fernley, J.A. 1990, MNRAS, 247, 684

Rood, R. T. 1973, ApJ, 184, 81

Rood, R. T. 1990, in Confrontation Between Stellar Pulsation & Evolution, ed. C. Cacciari & G. Clementini (Astron. Soc. Pac.: San Francisco), 11–21

Saad, S. M., Lee, S-G. 2001, JKAS, 34, 99

Salaris, M., Chieffi, A., Straniero, O. 1993, ApJ, 414, 580

Storm, J., Carney, B. W. & Beck, J. A. 1991, PASP, 103, 1264

van Albada, T. S. & Baker, N. 1971, ApJ, 169, 311

van Albada, T. S. & Baker, N. 1973, ApJ, 185, 477

Vandenberg, D. A., Swenson, F. J., Iglesias, C. A. Alexander, D. R., 2000, Apj, 532, 430 (VDB)

This preprint was prepared with the AAS LaTeX macros v4.0.

Table 1: Selected results for fundamental pulsating models at Z=0.001, Y=0.24, $M = 0.65M_{\odot}$, log$L/L_{\odot}$=1.61 and l/H_p=1.5.

T$_e$		M_U	M_B	M_V	M_I	M_K
6000(FRE)		1.242	1.265	0.814	0.179	-0.586
6100		1.207	1.229	0.802	0.194	-0.534
6300		1.149	1.164	0.781	0.225	-0.431
6500		1.104	1.104	0.761	0.258	-0.332
6700		1.067	1.050	0.744	0.292	-0.233
6900(FBE)		1.037	1.001	0.729	0.327	-0.139

T$_e$	P	$< M_U >$	$< M_B >$	$< M_V >$	$< M_I >$	$< M_K >$
6000	0.6598	1.246	1.265	0.819	0.188	-0.575
6100	0.6254	1.225	1.241	0.812	0.200	-0.540
6300	0.5626	1.163	1.168	0.787	0.239	-0.436
6500	0.5061	1.119	1.104	0.768	0.268	-0.342
6700	0.4567	1.077	1.043	0.759	0.317	-0.239
6900	0.4137	1.037	1.010	0.770	0.376	-0.137

T$_e$	P	(M_U)	(M_B)	(M_V)	(M_I)	(M_K)
6000	0.6598	1.253	1.273	0.823	0.190	-0.573
6100	0.6254	1.238	1.257	0.820	0.204	-0.537
6300	0.5626	1.187	1.198	0.804	0.239	-0.433
6500	0.5061	1.168	1.167	0.805	0.283	-0.338
6700	0.4567	1.164	1.156	0.824	0.341	-0.234
6900	0.4137	1.184	1.180	0.869	0.412	-0.131

T$_e$	P	A_U	A_B	A_V		A_K
6000	0.6598	0.438	0.466	0.349		0.182
6100	0.6254	0.636	0.690	0.528		0.269
6300	0.5626	0.850	0.958	0.740		0.285
6500	0.5061	1.064	1.206	0.963		0.331
6700	0.4567	1.552	1.703	1.335		0.334
6900	0.4137	1.967	2.003	1.557		0.408

Table 2: As in Table1, but for first-overtone pulsating models

T$_e$		M_U	M_B	M_V	M_I	M_K
6600(FORE)		1.085	1.076	0.752	0.275	-0.282
6700		1.068	1.050	0.744	0.293	-0.233
6800		1.051	1.024	0.736	0.310	-0.185
6900		1.037	1.000	0.728	0.327	-0.139
7000		1.024	0.977	0.722	0.346	-0.092
7100		1.012	0.955	0.716	0.364	-0.046
7200(FOBE)		1.001	0.934	0.711	0.383	0.000
T$_e$	P	$< M_U >$	$< M_B >$	$< M_V >$	$< M_I >$	$< M_K >$
6600	0.3558	1.100	1.091	0.762	0.277	-0.296
6700	0.3362	1.083	1.063	0.754	0.295	-0.251
6800	0.3211	1.066	1.036	0.747	0.315	-0.203
6900	0.3055	1.052	1.011	0.742	0.336	-0.155
7000	0.2921	1.036	0.986	0.738	0.357	-0.109
7100	0.2779	1.020	0.962	0.734	0.378	-0.059
7200	0.2663	1.008	0.941	0.727	0.396	-0.007
T$_e$	P	(M_U)	(M_B)	(M_V)	(M_I)	(M_K)
6600	0.3558	1.115	1.111	0.775	0.282	-0.295
6700	0.3362	1.109	1.097	0.775	0.304	-0.249
6800	0.3211	1.101	1.082	0.776	0.326	-0.201
6900	0.3055	1.092	1.066	0.776	0.349	-0.153
7000	0.2921	1.085	1.052	0.778	0.372	-0.106
7100	0.2779	1.073	1.033	0.776	0.394	-0.057
7200	0.2663	1.045	0.992	0.757	0.407	-0.005
T$_e$	P	A_U	A_B	A_V		A_K
6600	0.3558	0.521	0.599	0.473		0.189
6700	0.3362	0.680	0.778	0.618		0.217
6800	0.3211	0.830	0.962	0.756		0.218
6900	0.3055	0.891	1.035	0.807		0.216
7000	0.2921	1.039	1.192	0.919		0.217
7100	0.2779	1.045	1.187	0.916		0.191
7200	0.2663	0.843	0.971	0.745		0.149

Table 3: Average mass $< M(RR) >$ of synthetic RR Lyrae pulsators varying the mean mass $< M(HB >$ of HB stars, as inferred by SHB computations based on C03 models with Z=0.001 and $\sigma_{M(HB)}$=0.02 $M_{\odot}$. The HB-type and the fraction of variable stars $f(RR)$ are also listed. The predicted mass spread of statistically significant numbers of RR Lyrae pulsators ($f(RR) \geq 0.20$) is of the order of $\sim 0.02 M_{\odot}$. For very blue or very red HB types ($< M(RR) >$ values in italics), no reliable average mass can be derived.

$< M(HB >$ ($M_{\odot}$)	HB-type	$f(RR)$	$< M(RR) >$ ($M_{\odot}$)
0.62	+0.93	0.04	*0.64*
0.64	+0.72	0.18	*0.66*
0.65	+0.55	0.27	0.667
0.66	+0.38	0.35	0.669
0.67	+0.10	0.37	0.670
0.68	−0.19	0.40	0.673
0.69	−0.45	0.30	0.675
0.70	−0.72	0.21	0.679
0.72	−0.95	0.04	*0.69*

Table 4: Distance modulus (mag) of M3 as inferred from the different pulsational methods described in the text

Method	$DM(l/H_p$=1.5)	$DM(l/H_p$=2.0)
PMC	15.09±0.08	15.09±0.08
PMA	14.98±0.10	15.09±0.08
PM_K	15.08±0.06	15.08±0.06
FOBE	15.04±0.04	15.00±0.04
FRE	14.90±0.04	15.04±0.04

Fig. 1.— Period-magnitude-color relations of fundamental (F) and first-overtone (FO) pulsators with the labelled mass and luminosity. The plotted points are the models which are separated by 100K in the effective temperature.

Fig. 2.— Period-magnitude relations of fundamental (F) and first-overtone (FO) pulsators. Symbols as in Fig. 1.

Fig. 3.— Period-amplitude distribution of fundamental pulsators at l/H_p=1.5 (left panel) and various mass and luminosity (symbols as in Fig. 1). The right panel shows the predicted period-amplitude relations at l/H_p=1.5 and 2.0 (see text).

Fig. 4.— Color-amplitude distribution of of fundamental (F) pulsators at l/H_p=1.5 (left panel) and various mass and luminosity (ymbols as in Fig. 1). The right panel shows the predicted color-amplitude relations at l/H_p=1.5 and 2.0 (see text).

Fig. 5.— Comparison between static and mean magnitudes of fundamental (F) and first-overtone (FO) pulsators.

Fig. 6.— Comparison between static and mean colors of fundamental (F) and first-overtone (FO) pulsators.

Fig. 7.— Mass and luminosity of selected ZAHB models by C03 and VDB as a function of the effective temperature.

Fig. 8.— Mass and luminosity of selected ZAHB models by C03 as a function of the difference logT_e-FOBE and logT_e-FRE. The arrows depict the predicted limits of the instability region.

Fig. 9.— Mass of synthetic HB stars as a function of the effective temperature, normalized to FOBE, and varying the average mass $< M(HB) >$. The solid line is the ZAHB, while the dashed lines depict the edges of the pulsation region.

Fig. 10.— As in Fig. 8, but for the luminosity.

Fig. 11.— Absolute visual magnitude of C03 synthetic HB pulsators as a function of period. Left and right panel refers to first-overtone and fundamental pulsators, respectively. The solid lines (see the labelled relations) are the predicted edges of the instability strip, while the dashed lines depict their intrinsic dispersion.

Fig. 12.— Color-magnitude diagram of RR Lyrae stars in M3. The two panel refer to magnitude-weighted and intensity weighted values. Different symbols refer to different pulsation modes. The dashed line is drawn at 15.8 mag.

Fig. 13.— Difference between observed mean magnitudes and mean colors for RR Lyrae stars in M3. Symbols are the same as in previous figure apart from the filled triangle which labels the only deviating variable V82.

Fig. 14.— Color-amplitude diagram of RR_{ab} in M3 in comparison with the predicted relations under different assumptions on the mixing-length parameter.

Fig. 15.— Color-period diagram of RR Lyrae stars in M3 in comparison with the predicted edges of the instability strip at two different assumptions on the mixing-length parameter. Symbols as in Fig. 12. Variables V177 and V178 are discussed in the text.

Fig. 16.— Reduced period versus color for RR Lyrae stars in M3 (symbols as in Fig. 12), under two different assumptions on the distance modulus. The period of *c*-type variables has been fundamentalized and the the solid line depicts the predicted fundamental relation at constant mass. The resulting average mass $< M(RR >$ of RR Lyrae stars for the labelled distance modulus is given.

Fig. 17.— Near-infrared magnitudes of RR Lyrae stars in M3 as a function of period. The solid line is the predicted slope at constant mass and luminosity (see text).

Fig. 18.— Period-amplitude diagram of RR_{ab} in M3 in comparison with the predicted relations (solid lines) under different assumptions on the mixing-length parameter. The labelled distance moduli are the resulting values adopting an average mass $< M(RR) >$=0.67±0.02$M_{\odot}$

Fig. 19.— RR Lyrae stars in M3 in the V-log$P$ plane in comparison with the predicted edges of the instability strip at l/H_p=2.0, as corrected with the labelled distance modulus.

Fig. 20.— Color-magnitude diagram of RR Lyrae stars in M3. The solid line is the observed magnitude of the lower envelope.

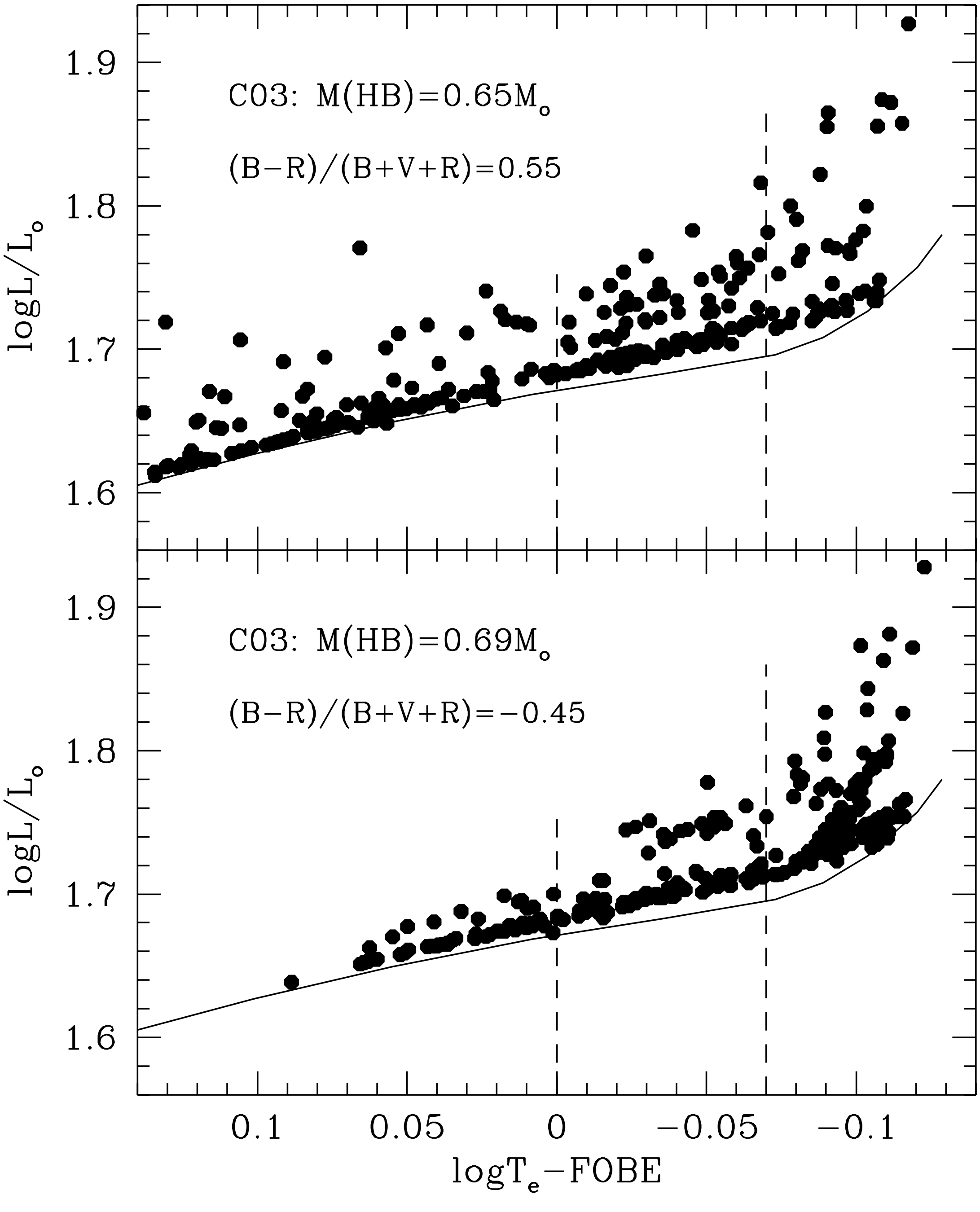
C03: M(HB)=0.65M$_o$
(B−R)/(B+V+R)=0.55
C03: M(HB)=0.69M$_o$
(B−R)/(B+V+R)=−0.45
logL/L$_o$
1.6
1.7
1.8
1.9
0.1
0.05
0
−0.05
−0.1
logT$_e$−FOBE

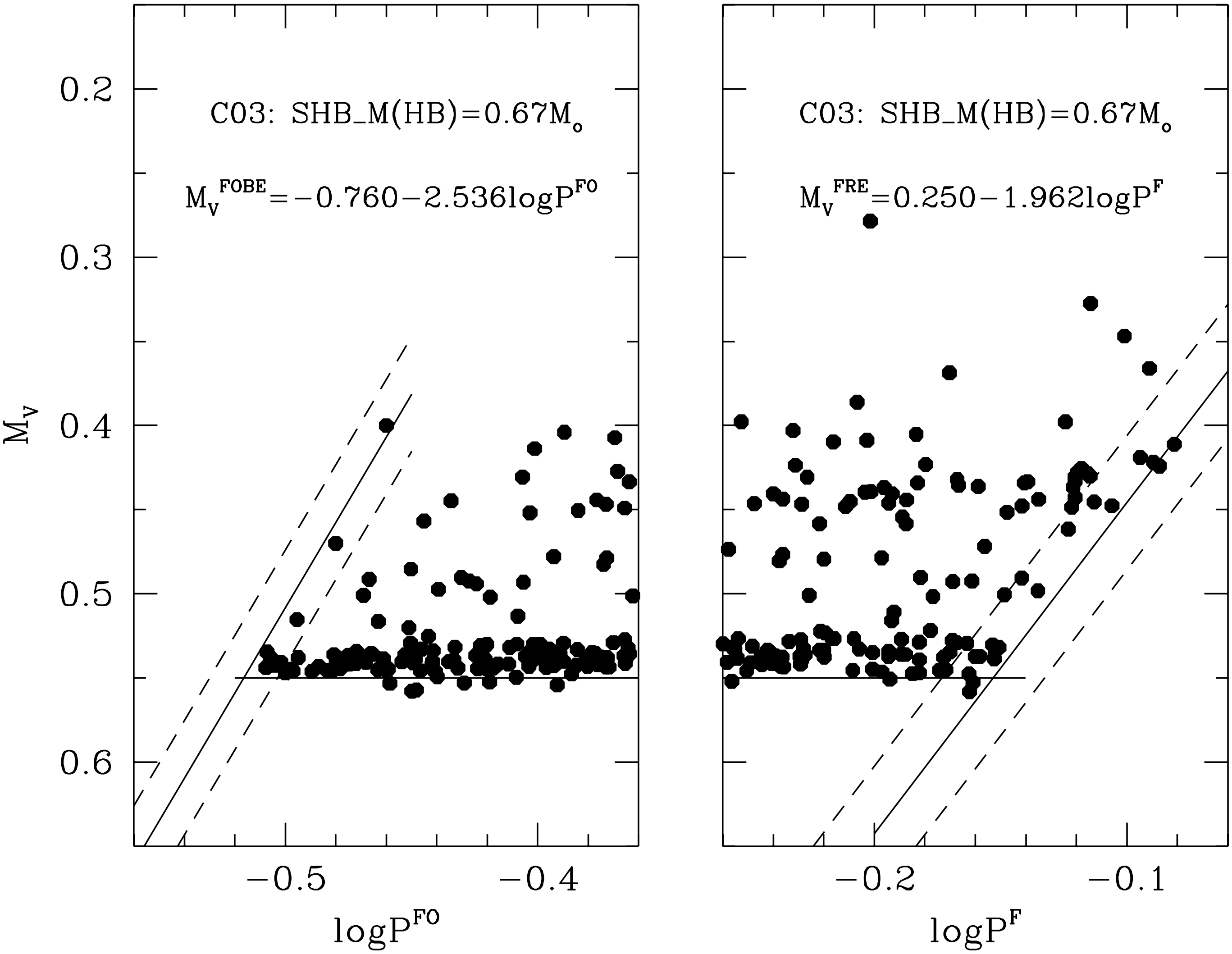
C03: SHB_M(HB)=0.67M$_o$
$M_V^{FOBE}=-0.760-2.536\log P^{FO}$
C03: SHB_M(HB)=0.67M$_o$
$M_V^{FRE}=0.250-1.962\log P^{F}$
M_V
0.2
0.3
0.4
0.5
0.6
−0.5
−0.4
$\log P^{FO}$
−0.2
−0.1
$\log P^{F}$

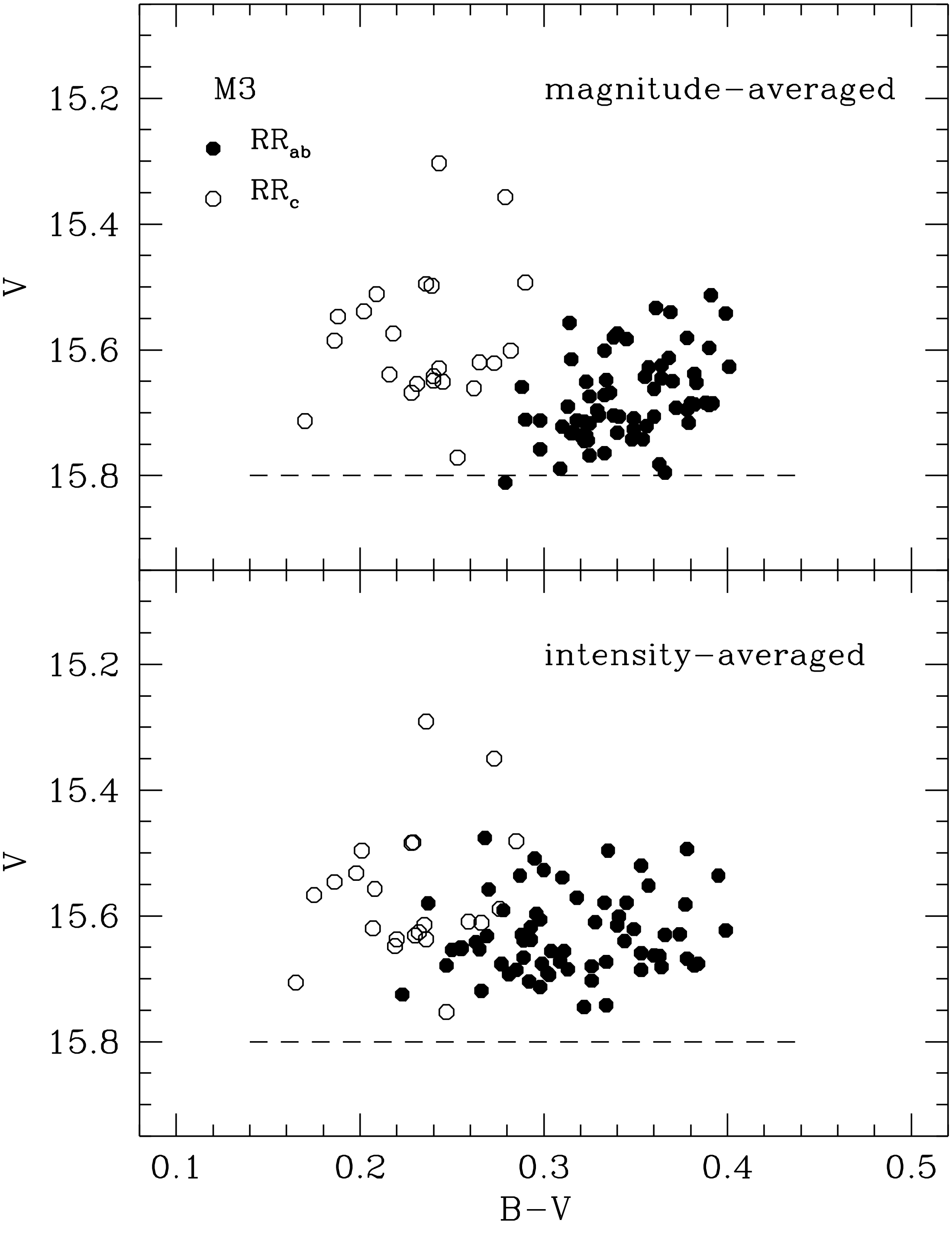
M3
RRab
RRc
magnitude−averaged
intensity−averaged
V
V
15.2
15.4
15.6
15.8
0.1
0.2
0.3
0.4
0.5
B−V

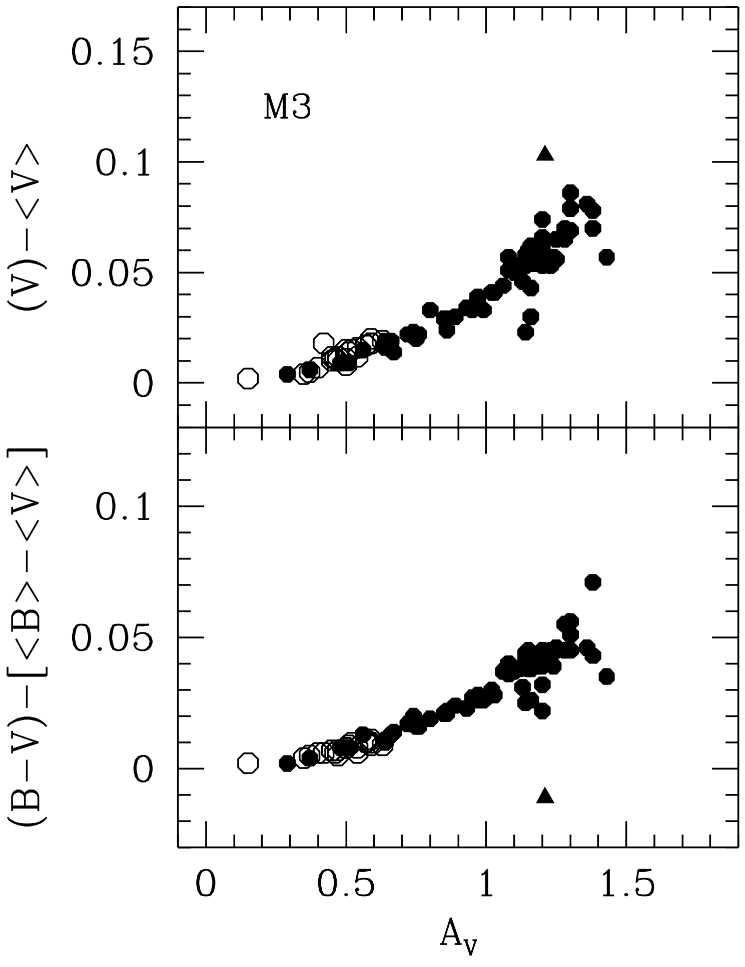
M3
(V)−<V>
0
0.05
0.1
0.15
(B−V)−[<B>−<V>]
0
0.05
0.1
0
0.5
1
1.5
A_V

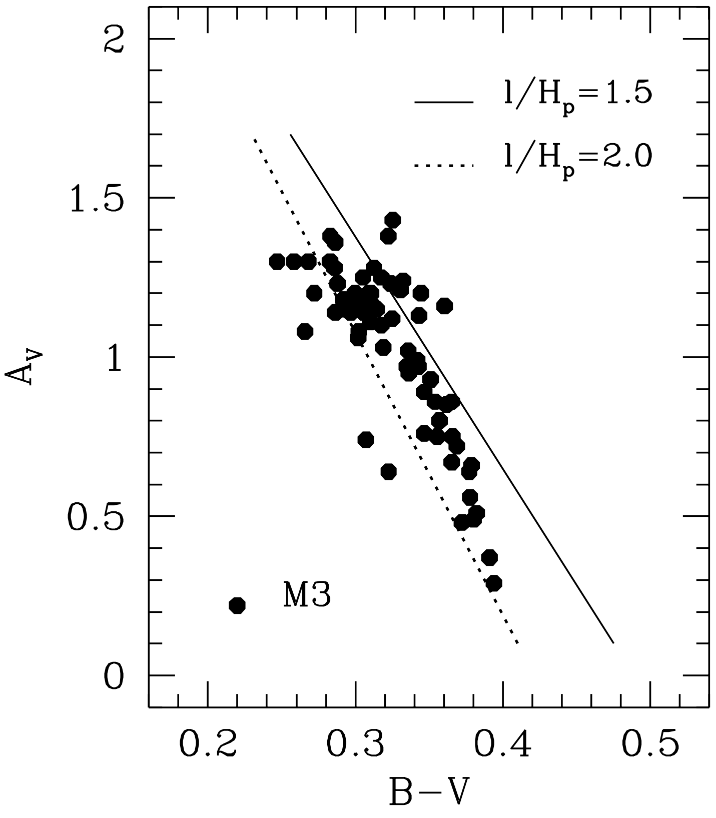

A_V
B−V
l/H_p=1.5
l/H_p=2.0
M3
0
0.5
1
1.5
2
0.2
0.3
0.4
0.5

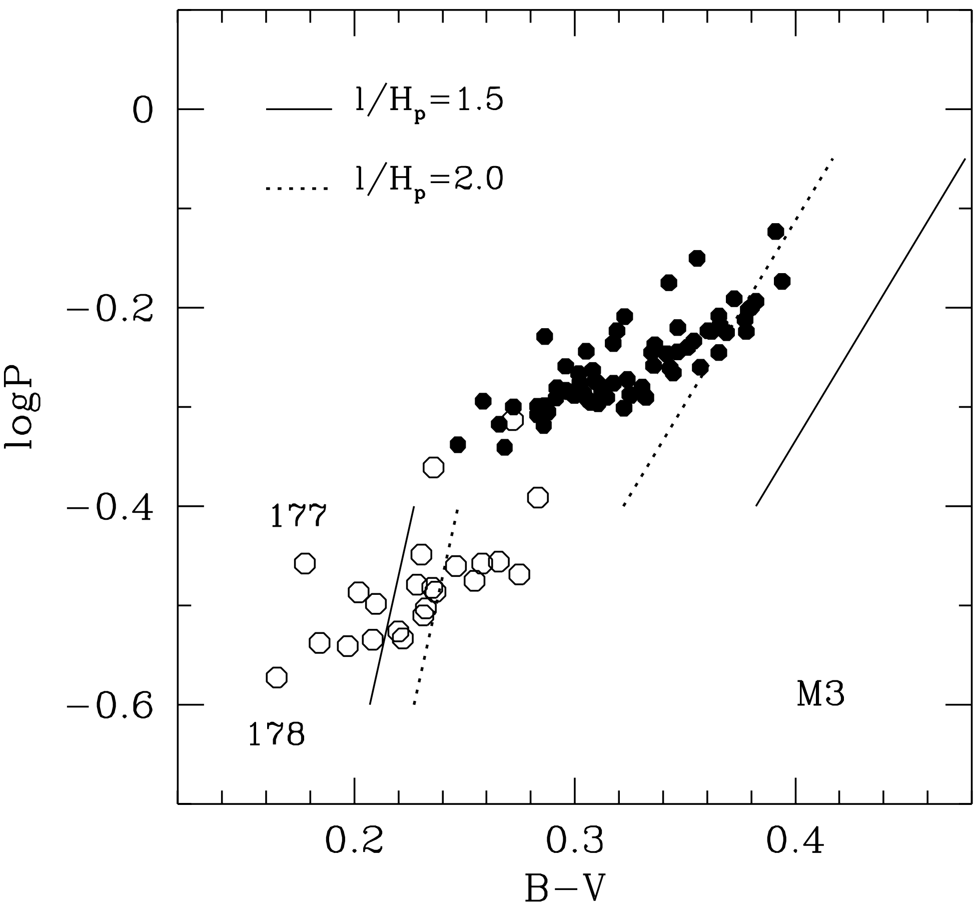

l/H$_p$=1.5
l/H$_p$=2.0
177
178
M3
logP
B−V
0
−0.2
−0.4
−0.6
0.2
0.3
0.4

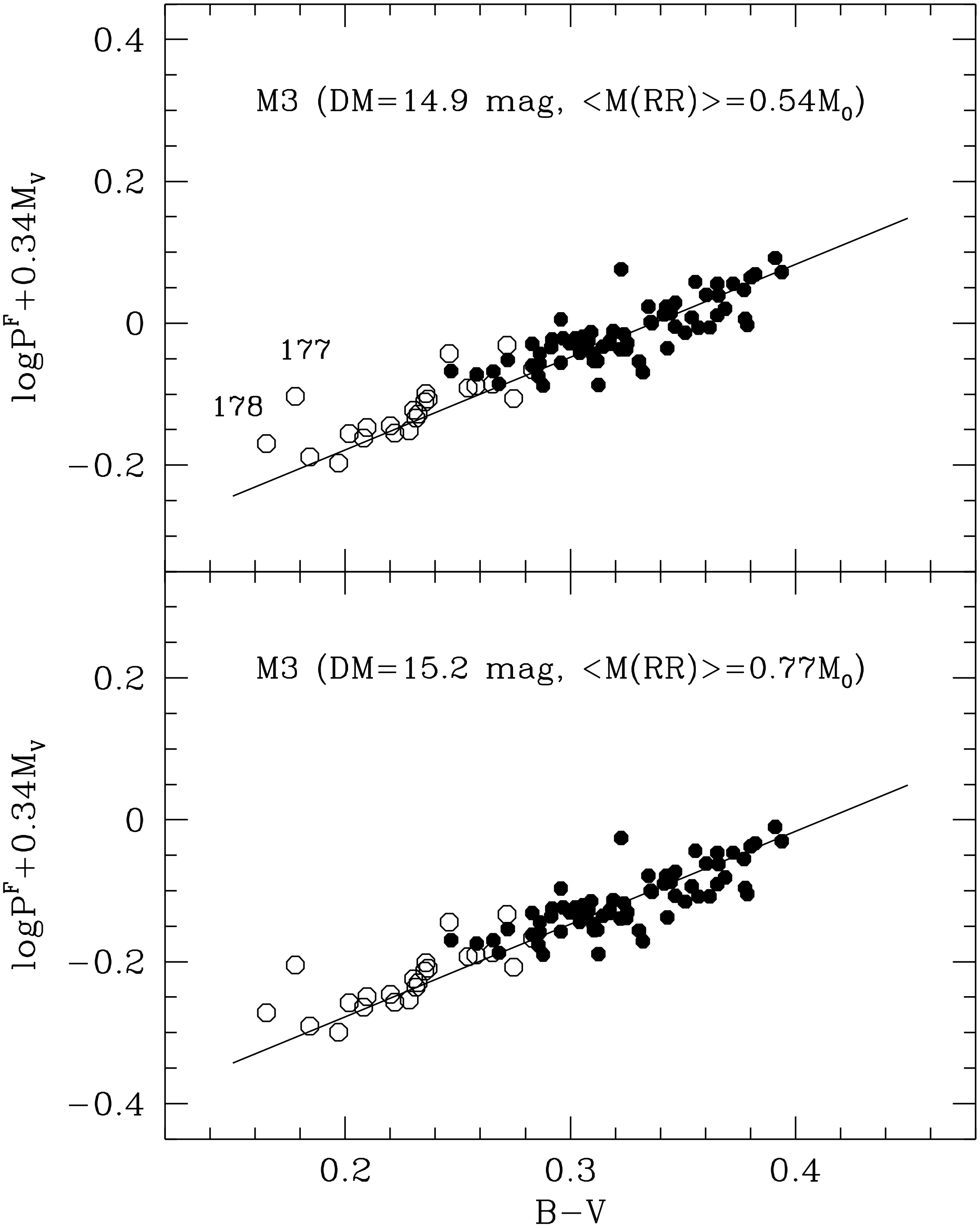
M3 (DM=14.9 mag, <M(RR)>=0.54M$_0$)
177
178
M3 (DM=15.2 mag, <M(RR)>=0.77M$_0$)
logP^F+0.34M$_V$
0.4
0.2
0
−0.2
−0.4
0.2
0.3
0.4
B−V

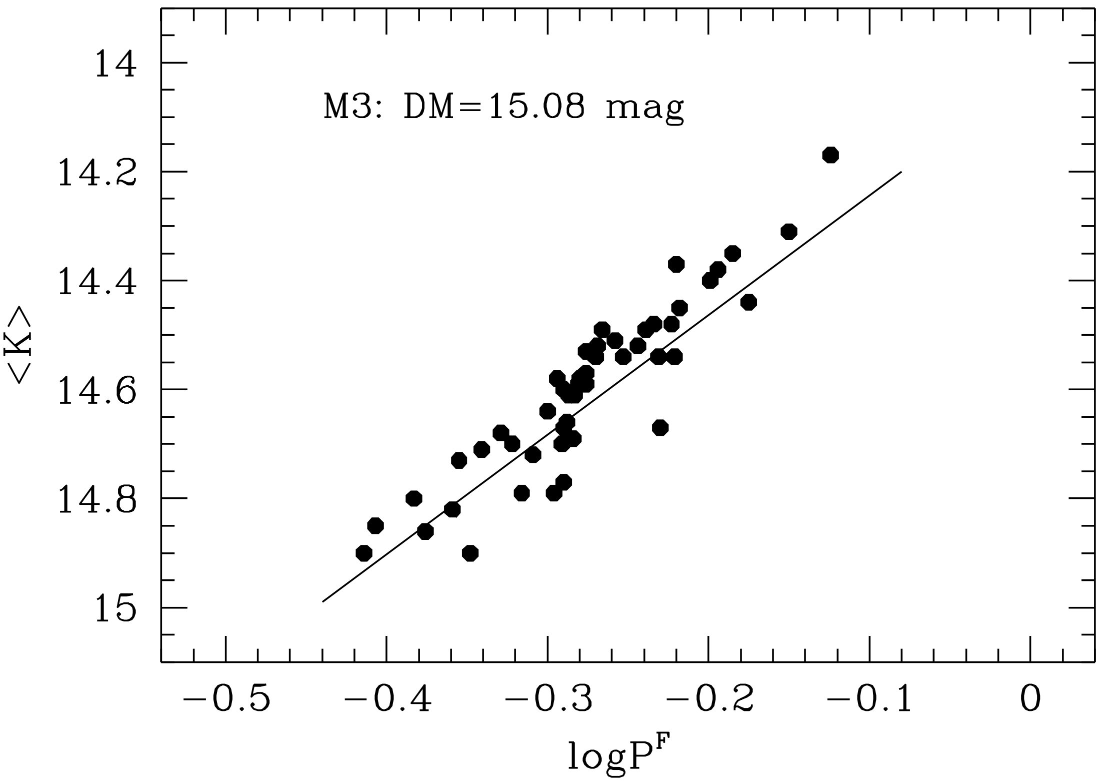
M3: DM=15.08 mag
<K>
14
14.2
14.4
14.6
14.8
15
−0.5
−0.4
−0.3
−0.2
−0.1
0
$\log P^F$

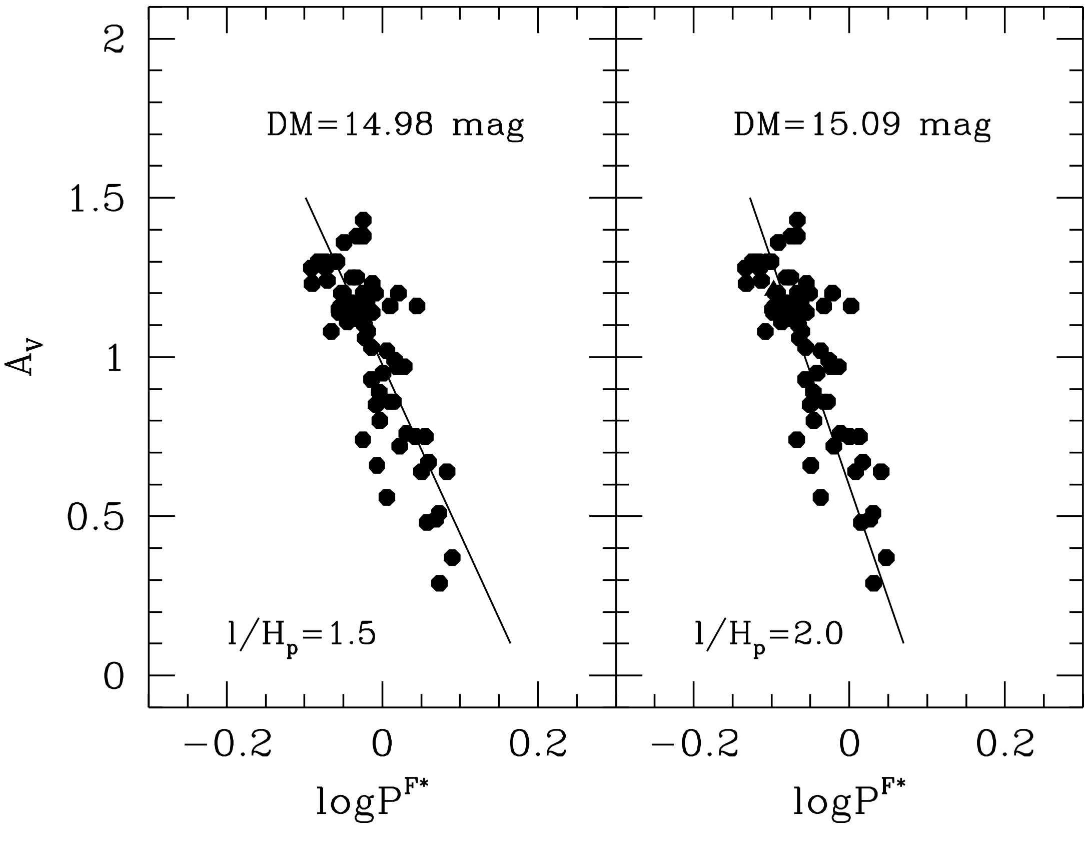
A_V
2
1.5
1
0.5
0
DM=14.98 mag
l/H_p=1.5
DM=15.09 mag
l/H_p=2.0
−0.2
0
0.2
logP^{F*}
−0.2
0
0.2
logP^{F*}

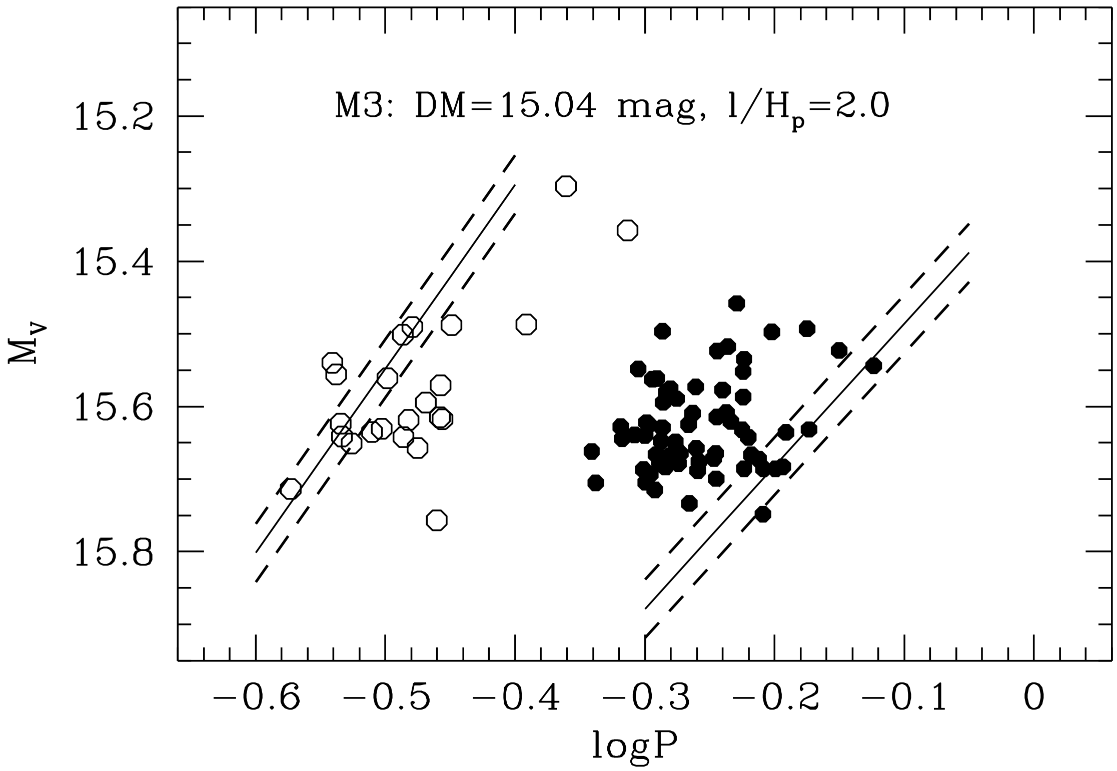
M3: DM=15.04 mag, l/H$_p$=2.0
M$_V$
15.2
15.4
15.6
15.8
logP
−0.6
−0.5
−0.4
−0.3
−0.2
−0.1
0

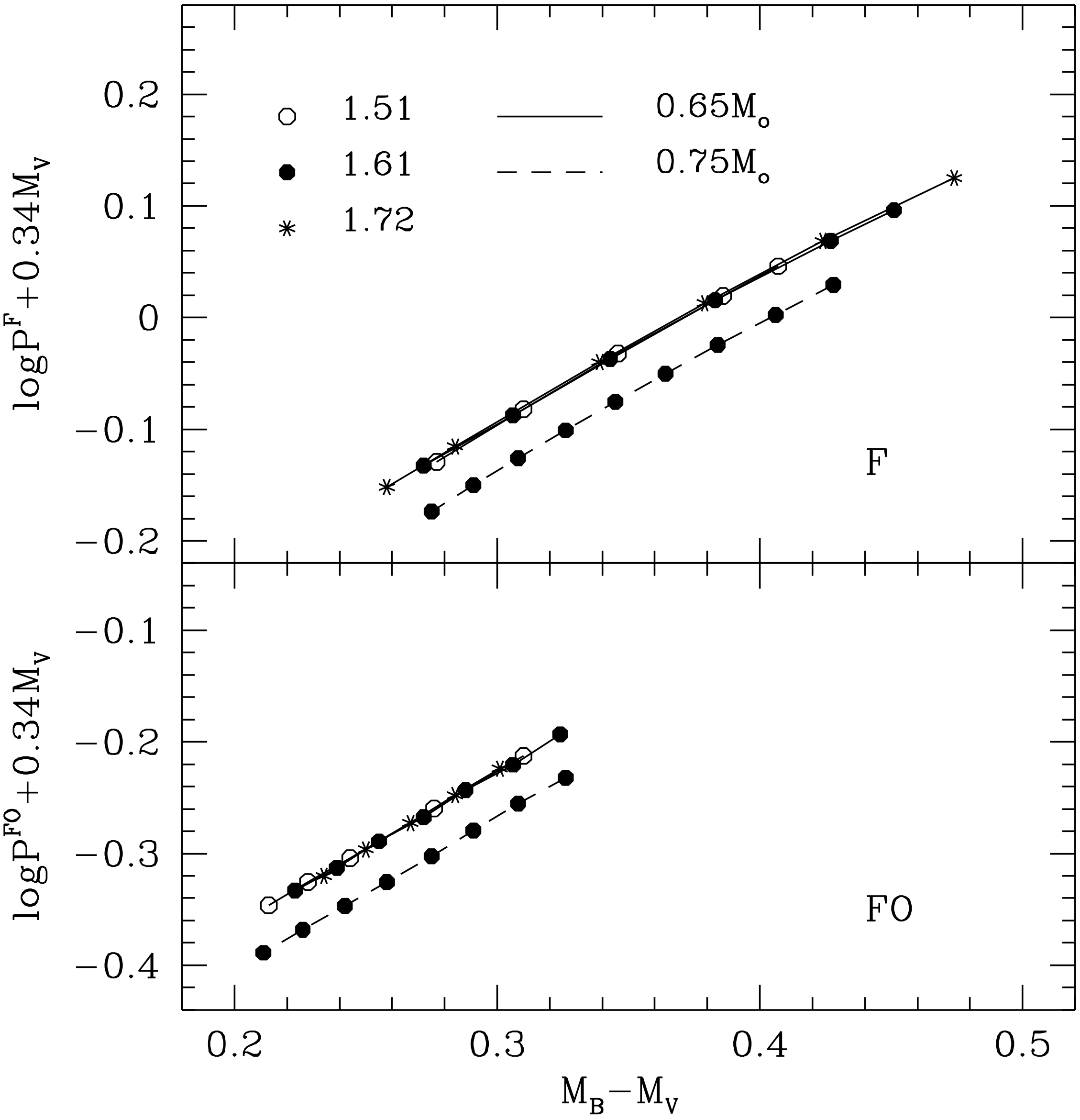

○ 1.51
● 1.61
* 1.72
0.65M$_o$
0.75M$_o$
F
FO
logP^F+0.34M$_V$
logP^{FO}+0.34M$_V$
M$_B$−M$_V$
0.2
0.1
0
−0.1
−0.2
−0.3
−0.4
0.2
0.3
0.4
0.5

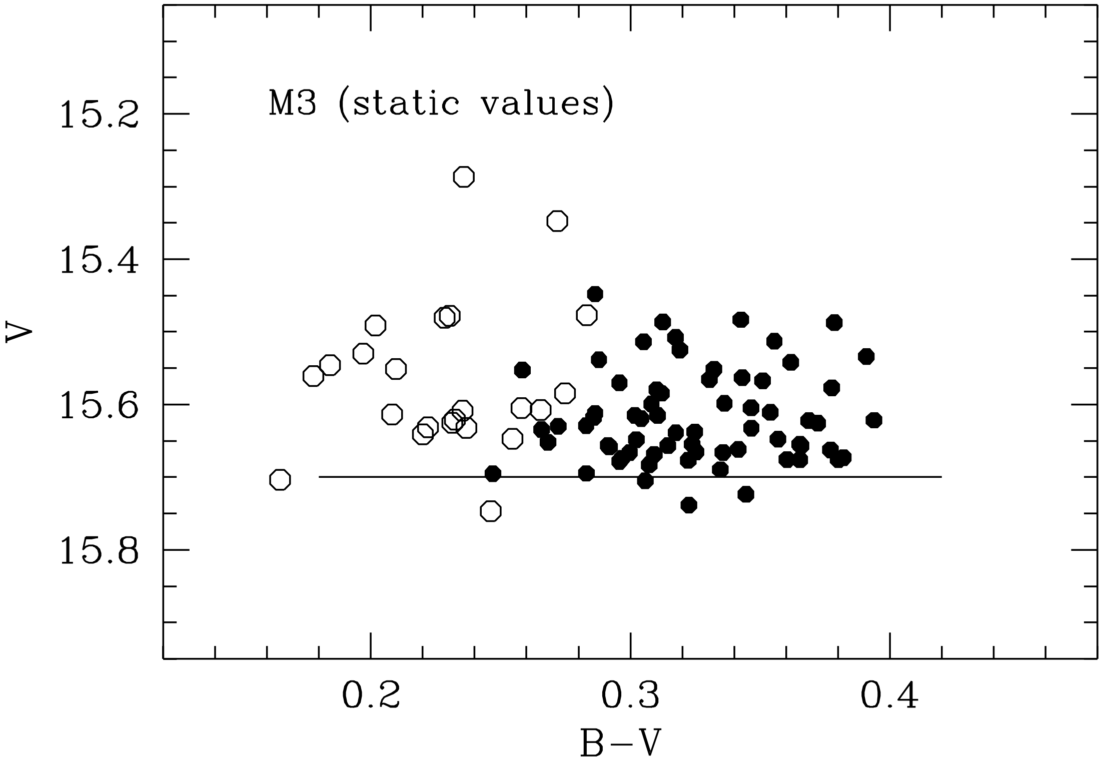
M3 (static values)
V
B−V
15.2
15.4
15.6
15.8
0.2
0.3
0.4

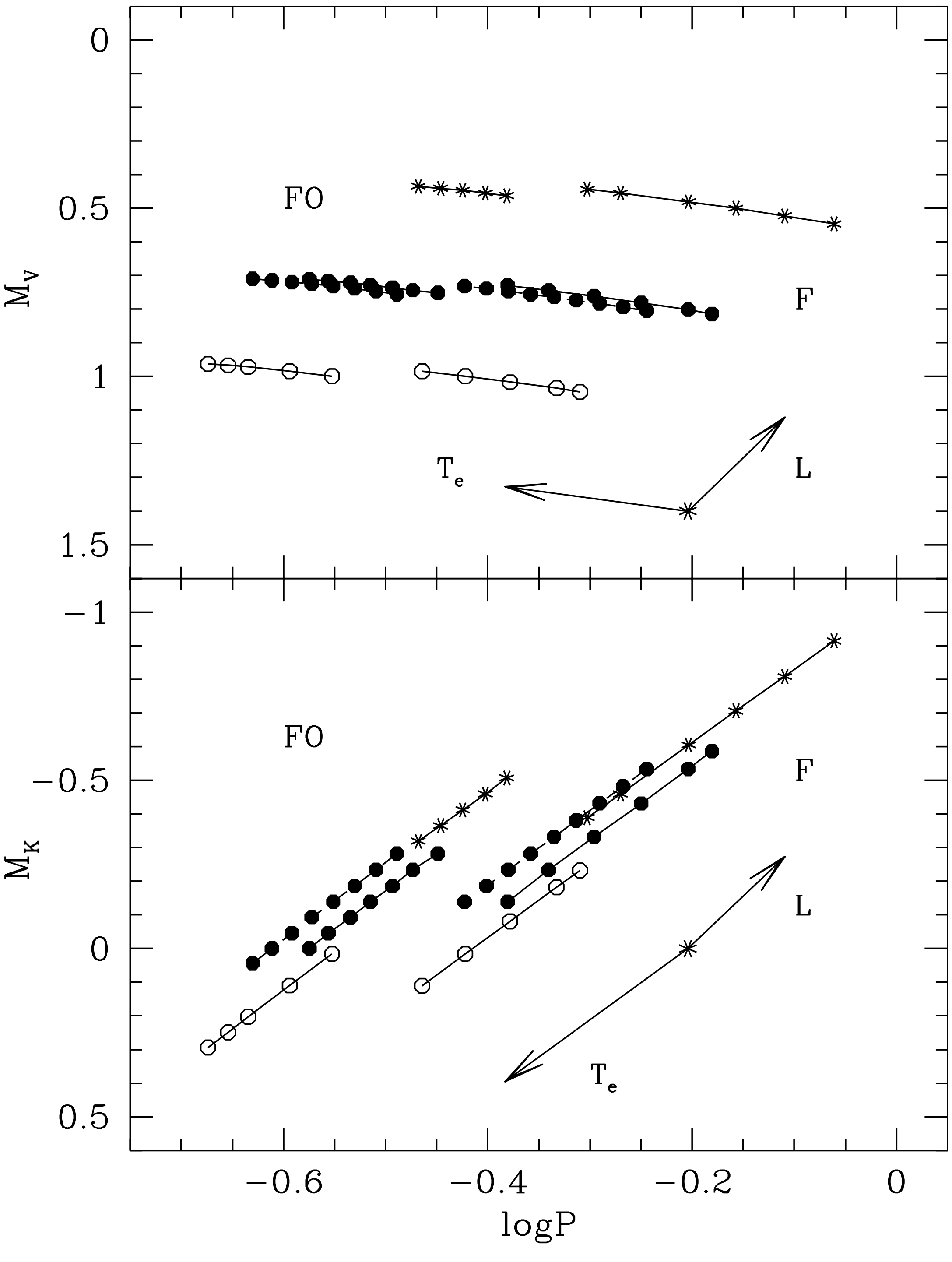

FO
F
L
T_e
M_V
M_K
logP
0
0.5
1
1.5
−1
−0.5
0
0.5
−0.6
−0.4
−0.2
0

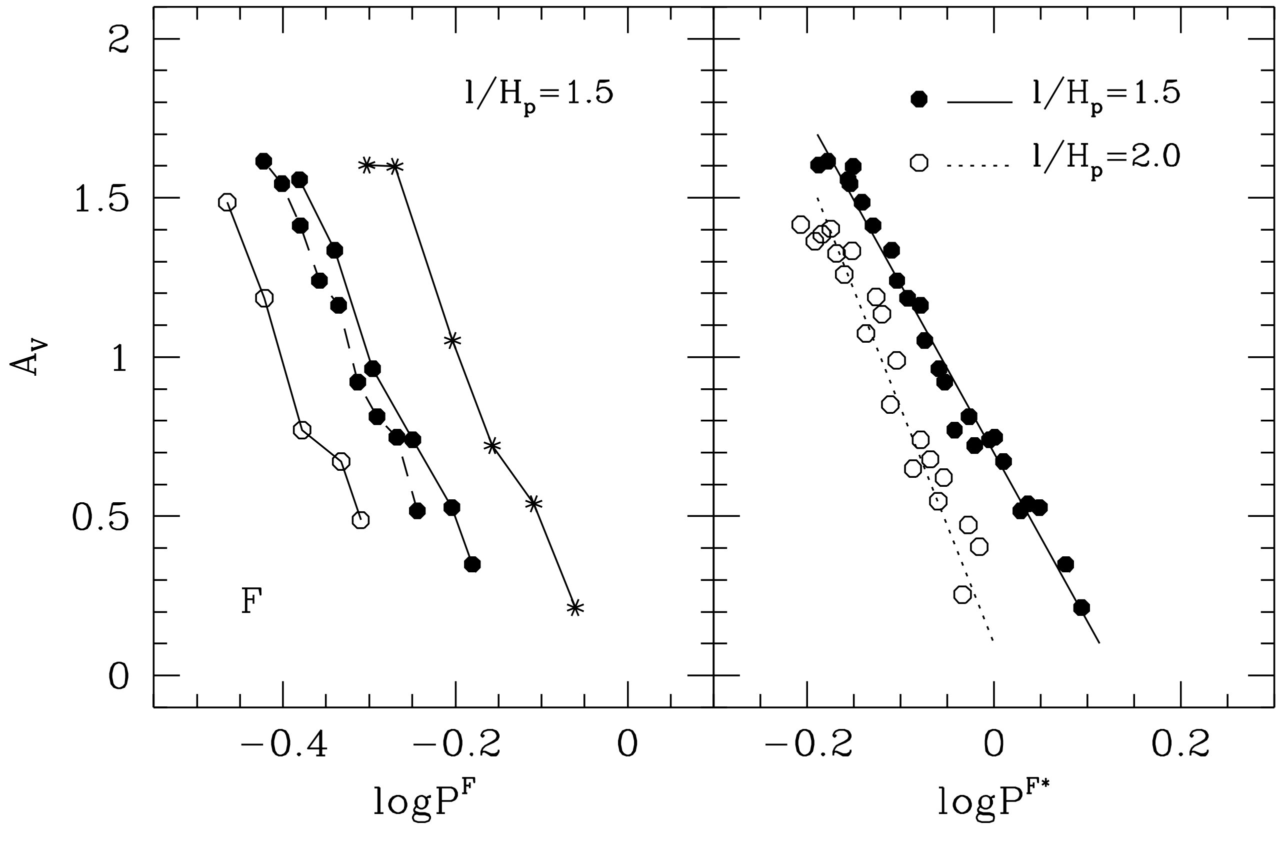

A_V
2
1.5
1
0.5
0
$l/H_p=1.5$
F
−0.4
−0.2
0
$\log P^F$
● —— $l/H_p=1.5$
○ ⋯⋯ $l/H_p=2.0$
−0.2
0
0.2
$\log P^{F*}$

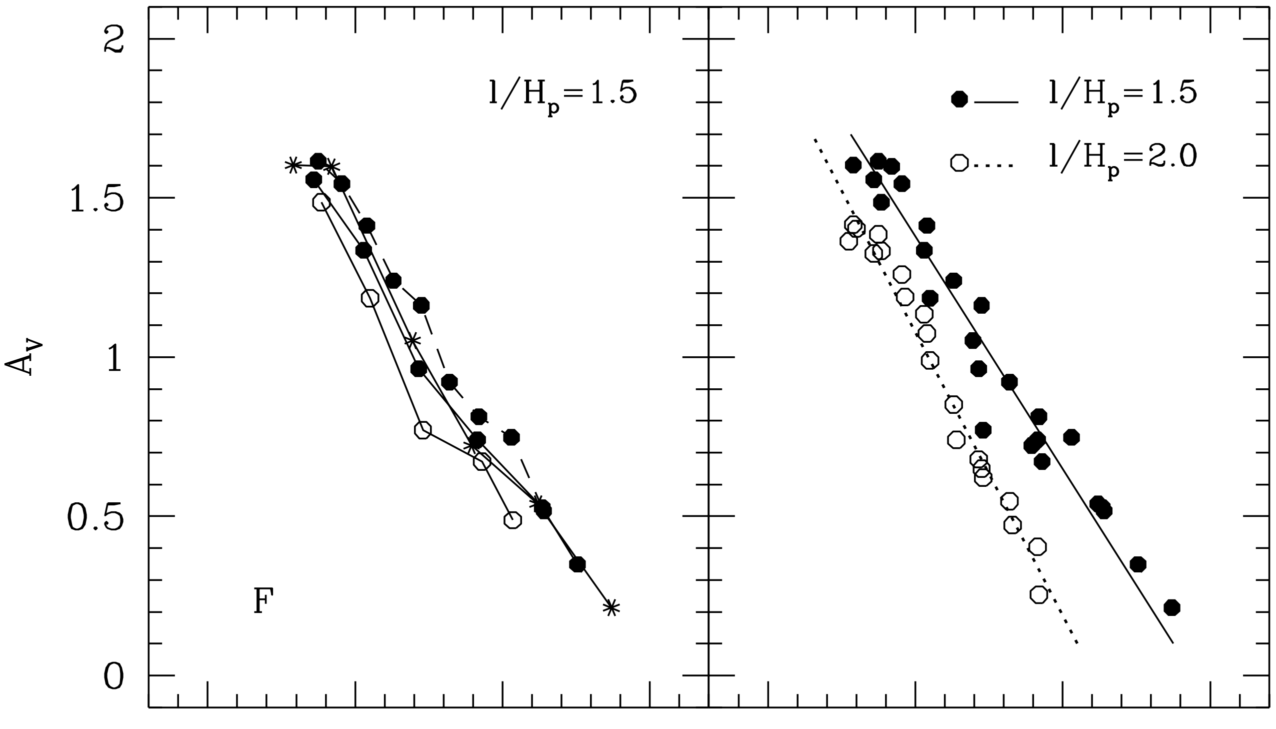

A_V
2
1.5
1
0.5
0
0.2
0.3
0.4
0.5
M_B−M_V
l/H_p=1.5
F
● —— l/H_p=1.5
○ ···· l/H_p=2.0

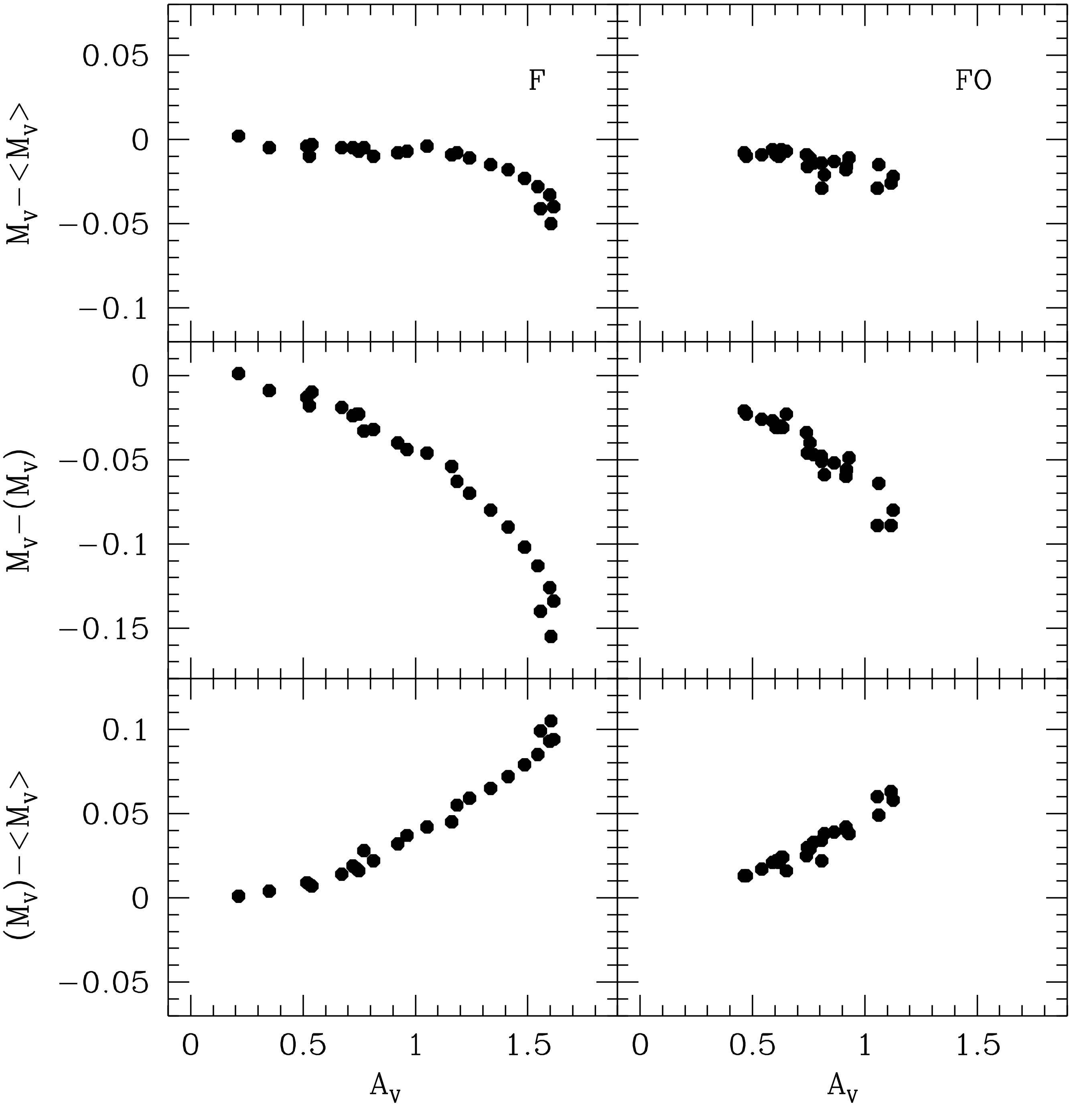
F
FO
$M_V - \langle M_V \rangle$
$M_V - (M_V)$
$(M_V) - \langle M_V \rangle$
0.05
0
−0.05
−0.1
−0.15
0.1
0
0.5
1
1.5
A_V
A_V

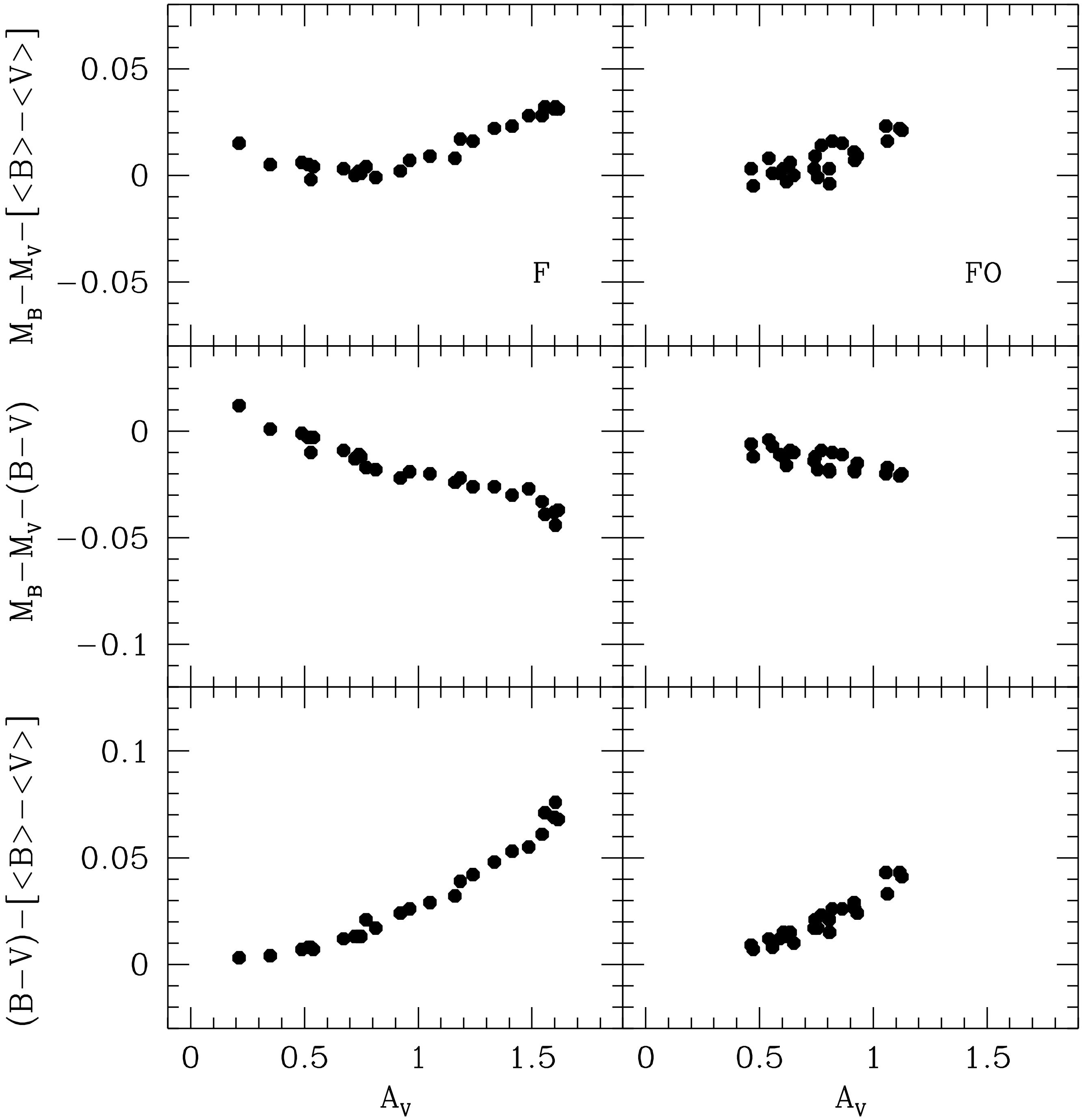

$M_B - M_V - [\langle B \rangle - \langle V \rangle]$
$M_B - M_V - (B-V)$
$(B-V) - [\langle B \rangle - \langle V \rangle]$
F
FO
0.05
0
−0.05
−0.1
0.1
0.5
1
1.5
A_V

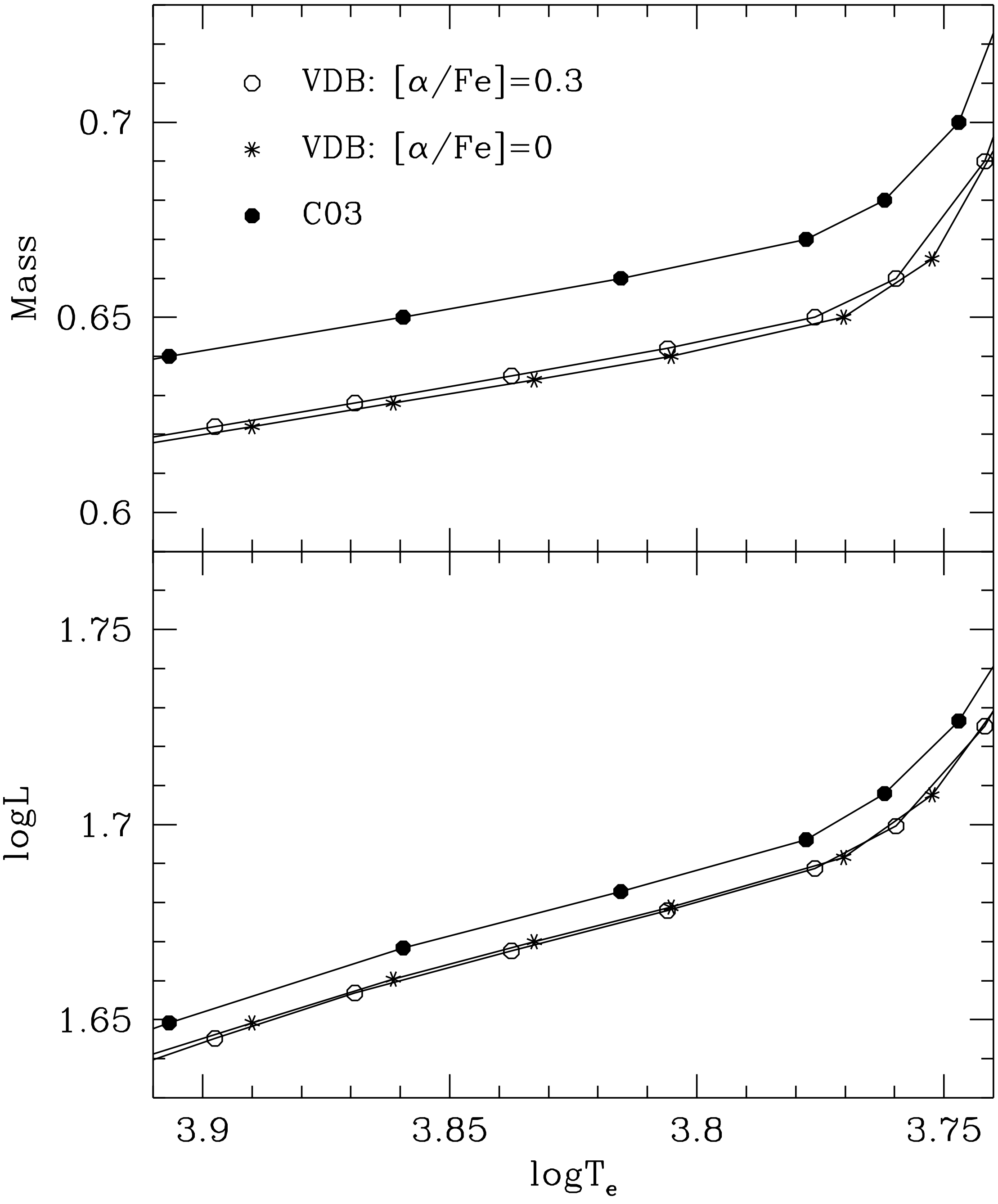
VDB: [α/Fe]=0.3
VDB: [α/Fe]=0
C03
Mass
0.7
0.65
0.6
logL
1.75
1.7
1.65
3.9
3.85
3.8
3.75
logT_e

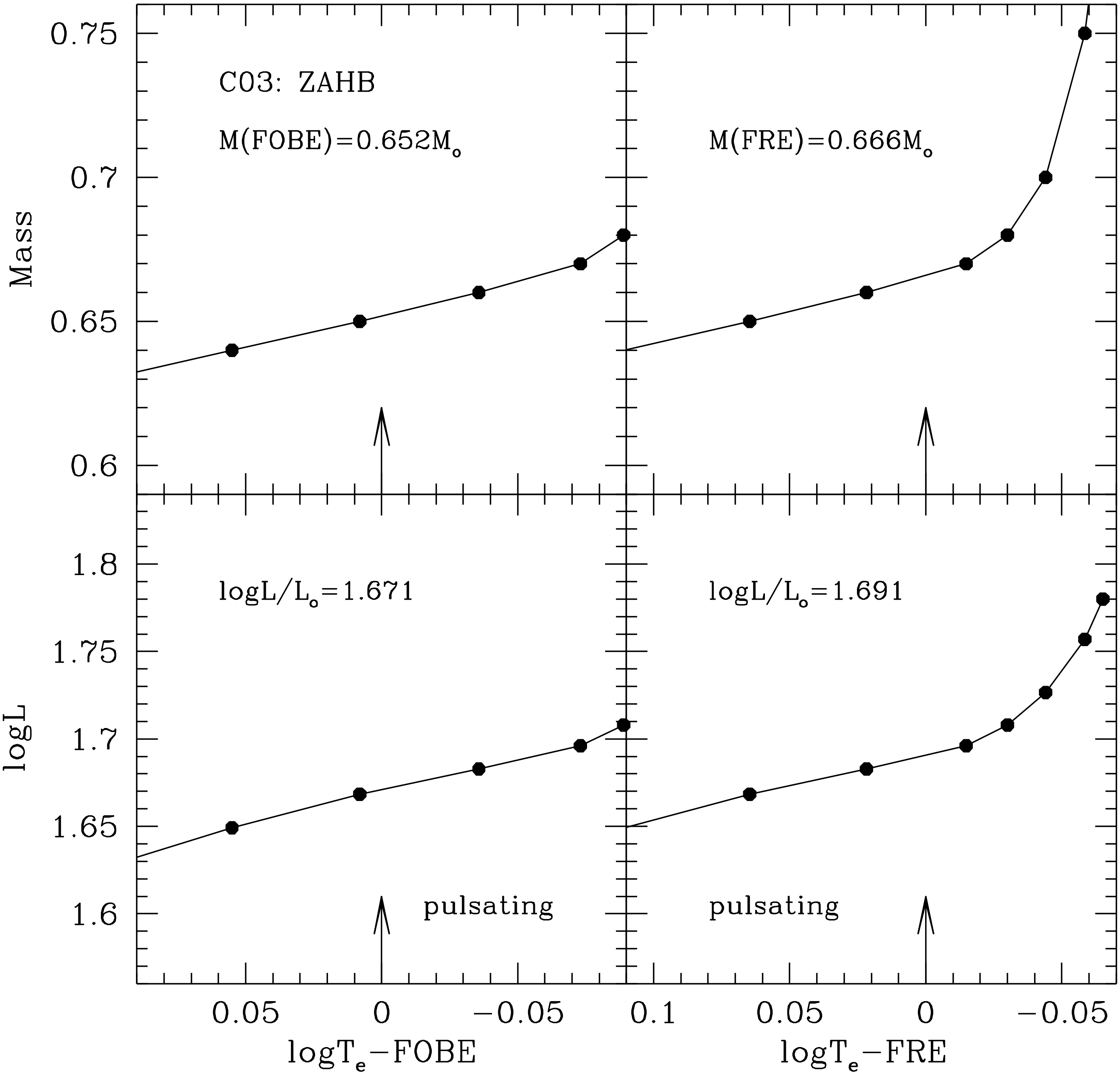
C03: ZAHB
M(FOBE)=0.652M$_o$
M(FRE)=0.666M$_o$
logL/L$_o$=1.671
logL/L$_o$=1.691
pulsating
pulsating
Mass
0.75
0.7
0.65
0.6
logL
1.8
1.75
1.7
1.65
1.6
0.05
0
−0.05
0.1
0.05
0
−0.05
logT$_e$−FOBE
logT$_e$−FRE

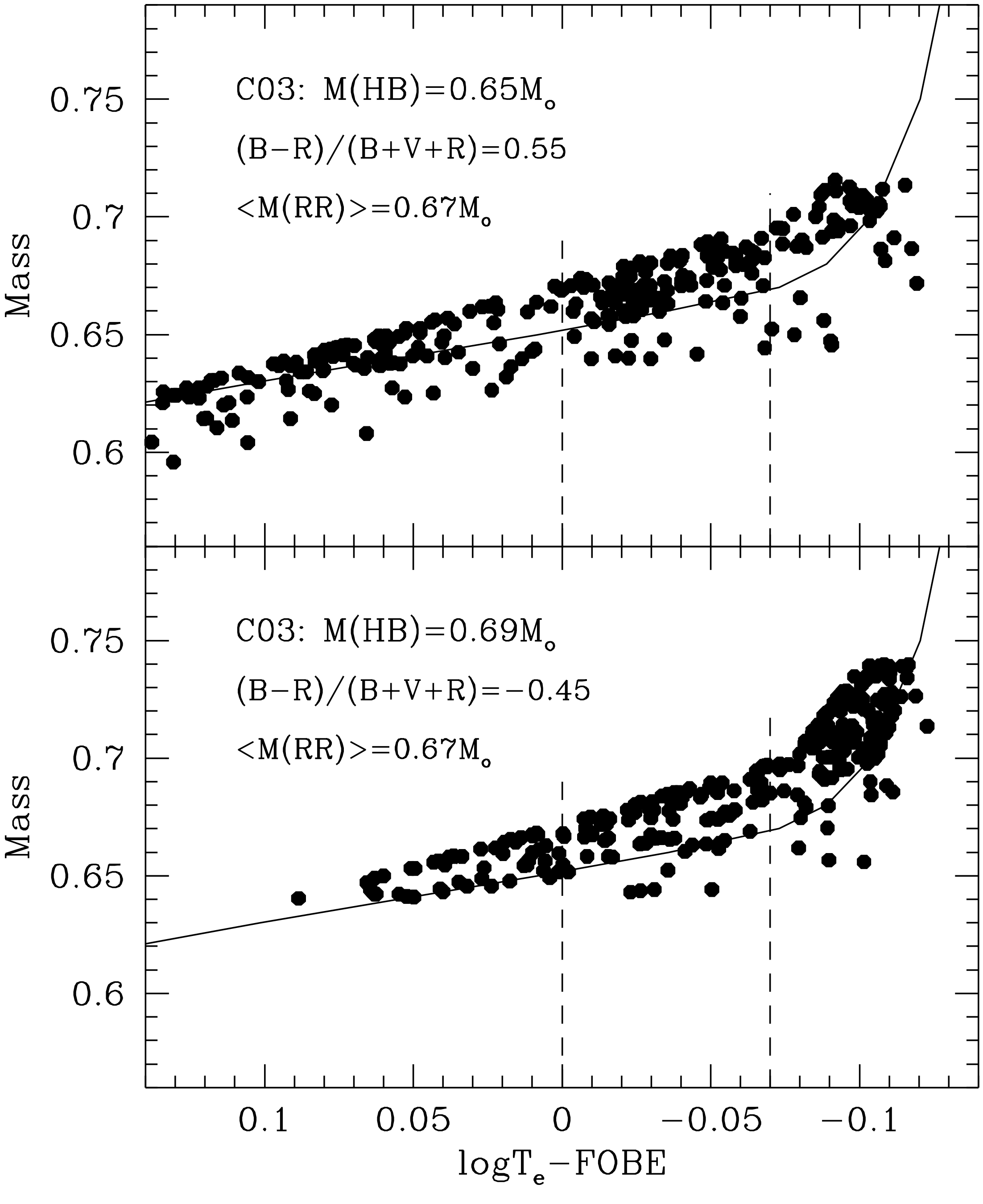
C03: M(HB)=0.65M$_\odot$
(B−R)/(B+V+R)=0.55
<M(RR)>=0.67M$_\odot$
C03: M(HB)=0.69M$_\odot$
(B−R)/(B+V+R)=−0.45
<M(RR)>=0.67M$_\odot$
Mass
Mass
0.75
0.7
0.65
0.6
0.1
0.05
0
−0.05
−0.1
logT$_e$−FOBE